Activation of Src Mediates PDGF-Induced Smad1 Phosphorylation and Contributes to the Progression of Glomerulosclerosis in Glomerulonephritis

Akira Mima[1,3], Hideharu Abe[1]*, Kojiro Nagai[1], Hidenori Arai[2], Takeshi Matsubara[3], Makoto Araki[3], Kazuo Torikoshi[3], Tatsuya Tominaga[1], Noriyuki Iehara[3], Atsushi Fukatsu[3], Toru Kita[4], Toshio Doi[1]

1 Department of Nephrology, Institute of Health Biosciences, University of Tokushima Graduate School, Tokushima, Japan, **2** Department of Geriatric Medicine, Kyoto University Graduate School of Medicine, Kyoto, Japan, **3** Department of Nephrology, Kyoto University Graduate School of Medicine, Kyoto, Japan, **4** Department of Cardiovascular Medicine, Kyoto University Graduate School of Medicine, Kyoto, Japan

Abstract

Platelet-derived growth factor (PDGF) plays critical roles in mesangial cell (MC) proliferation in mesangial proliferative glomerulonephritis. We showed previously that Smad1 contributes to PDGF-dependent proliferation of MCs, but the mechanism by which Smad1 is activated by PDGF is not precisely known. Here we examined the role of c-Src tyrosine kinase in the proliferative change of MCs. Experimental mesangial proliferative glomerulonephritis (Thy1 GN) was induced by a single intravenous injection of anti-rat Thy-1.1 monoclonal antibody. In Thy1 GN, MC proliferation and type IV collagen (Col4) expression peaked on day 6. Immunohistochemical staining for the expression of phospho-Src (pSrc), phospho-Smad1 (pSmad1), Col4, and smooth muscle α-actin (SMA) revealed that the activation of c-Src and Smad1 signals in glomeruli peaked on day 6, consistent with the peak of mesangial proliferation. When treated with PP2, a Src inhibitor, both mesangial proliferation and sclerosis were significantly reduced. PP2 administration also significantly reduced pSmad1, Col4, and SMA expression. PDGF induced Col4 synthesis in association with increased expression of pSrc and pSmad1 in cultured MCs. In addition, PP2 reduced Col4 synthesis along with decreased pSrc and pSmad1 protein expression in vitro. Moreover, the addition of siRNA against c-Src significantly reduced the phosphorylation of Smad1 and the overproduction of Col4. These results provide new evidence that the activation of Src/Smad1 signaling pathway plays a key role in the development of glomerulosclerosis in experimental glomerulonephritis.

Citation: Mima A, Abe H, Nagai K, Arai H, Matsubara T, et al. (2011) Activation of Src Mediates PDGF-Induced Smad1 Phosphorylation and Contributes to the Progression of Glomerulosclerosis in Glomerulonephritis. PLoS ONE 6(3): e17929. doi:10.1371/journal.pone.0017929

Editor: Sudha Agarwal, Ohio State University, United States of America

Received November 17, 2010; **Accepted** February 20, 2011; **Published** March 22, 2011

Funding: This research is supported by Grants-in-Aid for Scientific Research of the Japan Society for the Promotion of Science (no. 21591033 and 19590973). The funders had no role in study design, data collection and analysis, decision to publish, or preparation of the manuscript.

Competing Interests: The authors have declared that no competing interests exist.

* E-mail: abeabe@clin.med.tokushima-u.ac.jp

Introduction

Glomerulonephritis is usually progressive and remains an important cause of end stage renal disease. In sclerosing glomerulonephritis, accumulation of the extracellular matrix (ECM) is a critical process in progressive glomerular injuries [1,2]. Type IV collagen (Col4) is one of the most important components of the expanded ECM [3]. Moreover, smooth muscle α actin (SMA) is a known common molecular marker of phenotypic changes of mesangial cells (MCs) in many glomerular diseases. We previously reported that Smad1 participates in the development of glomerulosclerosis in experimental glomerulonephritis [4]. We also reported that Smad1 transcriptionally regulates the expression of Col4 and SMA [5,6]. However, the mechanisms by which Smad1 is activated in glomerulonephritis have not been fully elucidated.

Platelet-derived growth factor (PDGF) is known to be a critical mitogen for MCs in vitro and in vivo [1,7]. It is noteworthy that mice deficient for PDGF B or PDGF receptor show abnormal glomeruli due to a lack of MC development [8–11]. Several lines of evidence indicate that PDGF plays a key role in the development of glomerulosclerosis not only in experimental models but also in human glomerular diseases [12,13]. The introduction of a neutralizing anti-PDGF antibody has shown that both mesangial proliferation and glomerulosclerosis can be markedly ameliorated in a rat glomerulonephritis model [14]. Moreover, we previously showed that the development of glomerulosclerosis from mesangial proliferation is dependent on PDGF-induced Smad1 activation [4], but little is known concerning the regulatory mechanisms of Smad1 activation by PDGF in glomerulonephritis. c-Src is a ubiquitously expressed non-receptor protein-tyrosine kinase [15] that is involved in multiple pathways regulating cell growth, migration, and survival [16]. c-Src is also an important component of the PDGF signal transduction pathway [17]. Several reports have demonstrated that PDGF plays a key role in MC proliferation and glomerulopathy *in vivo* and *in vitro* [7,18,19]. Previously we demonstrated that Smad1 is phosphorylated by PDGF in MCs [4]. However, the exact role of c-Src in MCs as well as in glomerulonephritis remains unclear.

In the present study, we demonstrated that c-Src is activated in experimental proliferative glomerulonephritis and that the reduction of c-Src ameliorates the development of glomerulosclerosis by blocking of the Smad1 signal transduction pathway. We further

showed that c-Src plays an important role as a switch molecule for the activation of Smad1 downstream of PDGF signaling. These findings unveil the molecular mechanisms underlying the induction of MC proliferation and MC phenotype alteration, resulting in proliferative glomerulonephritis. Taking these results together, we hypothesized that the Src/Smad1 pathway may be critical in the pathogenesis of proliferative glomerulonephritis.

Materials and Methods

Animals

Full details of the animal experimental protocols were approved and ethical permission was granted by the Review Board of Kyoto University (Permit Number: Med Kyo 08508). We used age-matched male Wistar rats (8 to 12 weeks old, 180 to 200 g) bred at the Shimizu Laboratory Animal Center (Hamamatsu, Japan). The animals were housed under specific pathogen-free conditions at the Animal Facility of Kyoto University. Levels of serum creatinine and blood urea nitrogen were measured using a Hitachi Mode 736 autoanalyzer. The urinary albumin concentrations were measured from 24-h urine collections by Nephrat and Albuwell (Exocell), according to the manufacturer's protocols.

Cell culture experiments

A glomerular mesangial cell line was established from glomeruli isolated from normal 4-week-old mice (C57BL/6JxSJL/J) and was identified according to a method described previously [7]. The MCs were plated on 100-mm plastic dishes (Nunc) that were maintained in B medium (a 3:1 mixture of minimal essential medium/F12 modified with trace elements) supplemented with 1 mM glutamine, penicillin at 100 units/ml, streptomycin at 100 μg/ml, and 10% fetal calf serum (Irvine Scientific). The cells were passaged weekly with trypsin-EDTA. The cultured cells fulfilled the previously described criteria generally accepted for glomerular mesangial cells [20]. Stimulation with angiotensin II (Ang II) (Sigma), PDGF, PP2 (Calbiochem, Darmstadt, Germany), or olmesartan (Cosmo Bio, Tokyo, Japan) was carried out in DMEM containing 0.5% FCS at 37°C for the indicated times. A rat monoclonal anti-PDGFβ-receptor antibody (APB5) and its antagonistic effects on the PDGFβ-R signal transduction pathway in vitro have been described previously [4].

Constructs, transfection, and co-immunoprecipitation

Src cDNAs (pUSE Src wild type, pUSE Src kinase mutant, and empty vector) were obtained from Upstate Biotechnology, Inc. (Lake Placid, NY). MCs were transfected using FuGene6 (Roche, Mannheim, Germany) according to the manufacturer's protocol. After 48 h of transfection, the cells were washed with PBS, and 1 ml ice-cold lysis buffer (25 mM Tris-HCl pH 7.4, 100 mM NaCl, 2 mM EDTA, 0.5% Nonidet P-40, Complete protease inhibitors cocktail; Roche) was added. For co-immunoprecipitation assay, whole cell lysates were first pre-cleared with protein G–Sepharose (Amersham) and followed by incubation with anti-PDGFR antibody (Santa Cruz) for 3 h at 4°C. The immune complex was isolated and separated by SDS–PAGE and analyzed by Western bot analysis. Protein was detected using polyclonal rabbit anti-Src antibody (Cell Signaling Technology).

Histology and Immunohistochemistry

Tissues were fixed in Methyl Carnoy's solution and were paraffin-embedded. Multiple sections were prepared and stained with periodic acid silver methenamine (PASM) and periodic acid-Schiff's reagent (PAS). Immunohistochemical staining was performed with antibodies specific to Col4 (Progen) or SMA (Abcam), using an established avidin-biotin detection method (Vector Laboratories). Frozen sections were used for the detection of pSrc and pSmad1 (Cell Signaling Technology). Glomerular morphometry was evaluated in PASM-stained tissues. The glomerular surface area and the PASM-positive area/glomerular area (%) were measured using an image analyzer with a microscope (IPAP, Sumitomo Chemical, Osaka, Japan) as previously described [21–24]. To quantitatively measure the expression of pSrc and pSmad1, pSrc-positive or pSmad1-positive cells/DAPI-positive nuclei were counted, and the mean percentages of pSrc-positive or pSmad1-positive cells were calculated. An investigator scored sections in a blinded fashion, according to an established scoring system (range 0–4; 0, no ECM deposition; 4, ECM deposition in all sections of the glomeruli) to semiquantify the localization of Col4 and SMA.

Small-interfering RNA

MCs (0.5×10^5) were seeded into 12-well plates (Nunc) and were grown until they were 60% to 80% confluent. The small-interfering RNAs (siRNAs) for c-Src, Smad1, and LRP1 (Dharmacon) or control scrambled siRNA (Dharmacon) were combined with DharmaFECT transfection reagent (Dharmacon), and the cells were transfected according to the recommended protocol with siRNA (100 nM final concentration). After 48 h of transfection, cells were starved in DMEM containing 0.5% BSA before treatment. After 48 h of incubation, the cells were stimulated with or without PDGF (Calbiochem).

TGFβ-neutralizing antibody assay

MCs were resuspended at a concentration of 1×10^6 cells/ml and plated onto 100-mm dish either in the presence of 10 μg/ml TGFβ-neutralizing antibody (R&D Systems) or a control normal chicken IgY. After 24 h of incubation, the cells were treated with PDGF for additional 12 h and were harvested and underwent protein extraction on Western blotting.

Western blotting

Isolated glomerular MCs were suspended in RIPA buffer (50 mM Tris, pH 7.5, 150 mM NaCl, 1% Nonidet P-40, 0.25% SDS, 1 mM Na_3VO_4, 2 mM EDTA, 1 mM phenylmethylsulfonyl fluoride, 10 mg/ml of aprotinin) and incubated for 1 h at 4°C. After centrifugation, the supernatants were used as total cell lysates. Twenty micrograms of each sample was applied to SDS-PAGE. After electrophoresis, the proteins were transferred to nitrocellulose filters (Schleicher & Schuell). The blots were subsequently incubated with anti-phospho-Smad1, anti-phspho-Src (Cell Signaling Technology), anti-SMA, anti-LRP1 (Abcam) or anti-Col4 antibody (Progen), followed by incubation with horseradish peroxidase-conjugated goat anti-rabbit IgG and sheep anti-mouse IgG (Amersham). The immunoreactive bands were visualized using horseradish peroxidase-conjugated secondary antibody and the enhanced chemiluminescent system (Amersham). These bands were quantified using an imaging densitometer (Science Lab 99 Image Gauge, Fujifilm, Tokyo, Japan).

Data analysis

The data are expressed as the mean ± S.D. Comparison among more than two groups was performed by one-way analysis of variance (ANOVA), followed by post hoc analysis (Bonferroni/Dunn test) to evaluate the statistical significance between the two groups. All analyses were performed using StatView (SAS Institute, Cary, NC). Statistical significance was defined as $P<0.05$.

Results

Glomerular phosphorylation of c-Src and Smad1 parallels the progress of glomerulosclerosis in rat Thy1 GN

We utilized a model of mesangial proliferative glomerulonephritis, known as anti-Thy1-induced glomerulonephritis (Thy1 GN), which exhibits sclerosis in the glomeruli. The renal function of Thy1 GN on day 6 was significantly decreased (Figure S1A). MC proliferation began on day 3 and glomerulosclerosis began on day 6. Renal damage clearly regressed until day 15. Sclerosis in the kidney peaked on day 6 and sclerotic changes subsided until day 15 (Figure 1A and B). Localization of phospho-Src (pSrc) and phospho-

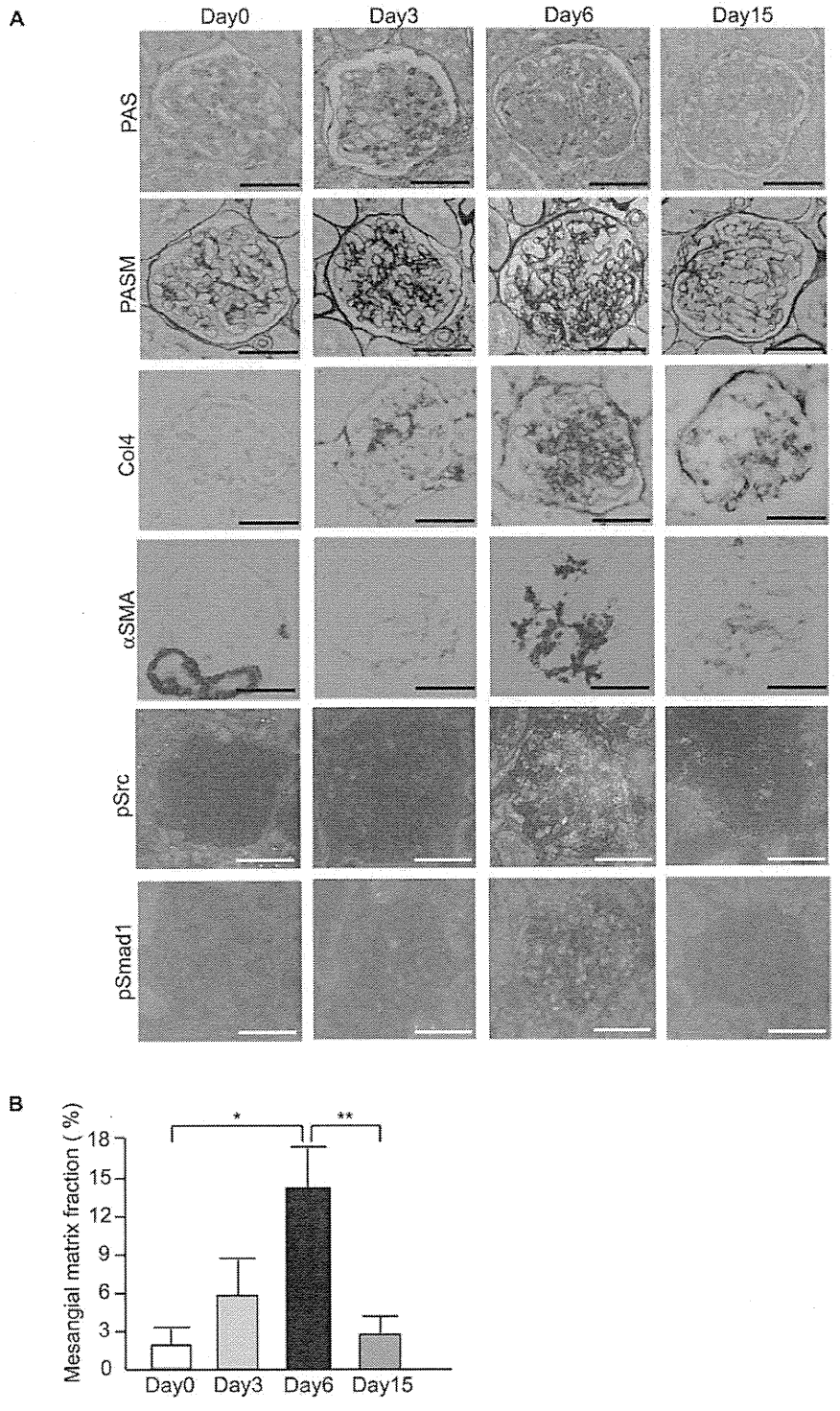

Figure 1. Induction and activation of c-Src and Smad1 in proliferative glomerulonephritis. (A) Representative light-microscopic appearance and immunohistochemistry of glomeruli in Thy1 GN. Scale bars = 100 μm. (B) Quantitative assessment of PASM staining in Thy1 GN. *$P = 0.002$, **$P = 0.002$).
doi:10.1371/journal.pone.0017929.g001

Smad1 (pSmad1) in the nuclei was scant on day 0. On day 3, phosphorylation began in c-Src and Smad1 proteins. The level of phosphorylation gradually increased and positively stained nuclei in parallel with the activity of mesangial proliferation during the development of glomerulosclerosis. Phosphorylation peaked on day 6 and then decreased towards day 15 (Figure 2, C, D and E). Phosphorylation of c-Src and Smad1 was almost undetectable on day 0 but became prominent during the proliferative stages in Thy1 GN, peaked on day 6, and then decreased towards day 15 (Figure 2C, D and E). In addition, the expression of Col4 and SMA changed in parallel with the activation of c-Src and Smad1 (Figure 2A, B and E). These data suggest that both Smad1 and c-Src are activated in the course of proliferative injuries in rat kidneys.

PP2 preserves renal function and attenuates glomerulosclerosis in rat glomerulonephritis

To investigate whether the c-Src/Smad1 pathway plays a pivotal role in developing glomerulosclerosis, we administered a Src specific inhibitor, PP2, to Thy1 GN rats from days 0 to 6 and assessed glomerulosclerosis on day 6. Untreated Thy1 GN rats showed an increased degree of glomerulosclerosis, whereas glomerulosclerosis was significantly decreased in the PP2-treated group (Figure 3A, B), along with renal function (Figure 3, C–E).

PP2 represses the activation of Smad1 and the expression of both Col4 and SMA in rat glomerulonephritis

Next, to examine the effect of PP2 on the morphological changes seen in Thy1 GN glomerulosclerosis, we examined Col4 and SMA expression in the two groups. PP2 treatment significantly inhibited Col4 and SMA expression, whereas expression was increased in the non-treatment group (Figure 3F). Moreover, we examined whether PP2 affected the phosphorylation and translocation of c-Src and Smad1 in Thy1 GN rats. PP2 treatment inhibited the phosphorylation of c-Src and Smad1, and their expression was localized in the nucleus in untreated Thy1 GN (Figure 3F). These data from immunohistochemistry were confirmed by Western blot analysis (Figure 3G).

Effect of PP2 on PDGF-mediated signaling in MCs

Because PDGF is well known to play a key role in the development of glomerulosclerosis, we investigated whether PDGF can activate c-Src/Smad1 signal transduction and increase the synthesis of Col4. Expression of Col4, pSrc, and pSmad1 was induced by PDGF stimulation in MCs cultured for 12 hours (Figure 4A–D). These inductions were inhibited by PP2 treatment

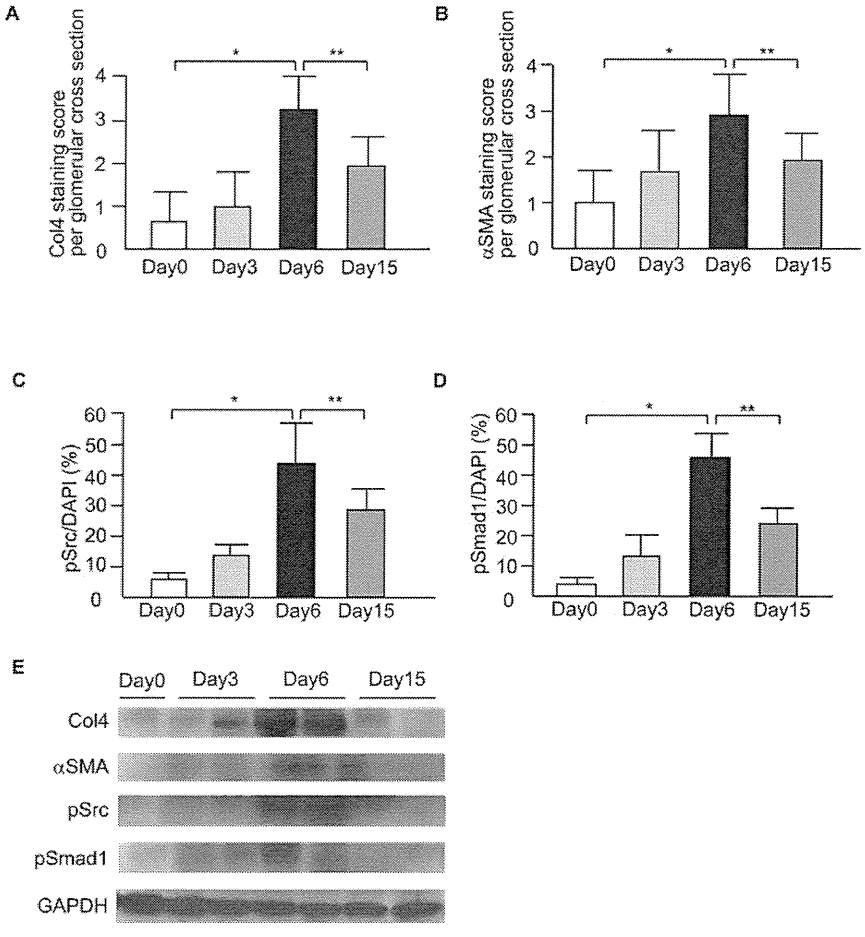

Figure 2. Time course of glomerular expression of Col4, SMA, pSrc and pSmad1 in Thy1 GN. (A, B) Staining scores per glomerular cross-section for Col4 (*$P<0.001$, **$P<0.001$) and SMA (*$P<0.001$ and **$P=0.009$) were calculated. Data represent mean values ± S.D. of at least three independent experiments; n = 6 for each experimental group. (C, D) Quantification of glomerular pSrc and pSmad1 by optical densitometry. The pSrc-positive nuclei and pSmad1-positive nuclei were counted in 10 consecutive fields in each specimen and normalized by the number of DAPI-positive nuclei. *$P<0.001$, **$P<0.001$. (E) Western blot for the glomerular lysates from each group. Data represent mean values ± S.D. of at least three independent experiments; n = 6 for each experimental group.
doi:10.1371/journal.pone.0017929.g002

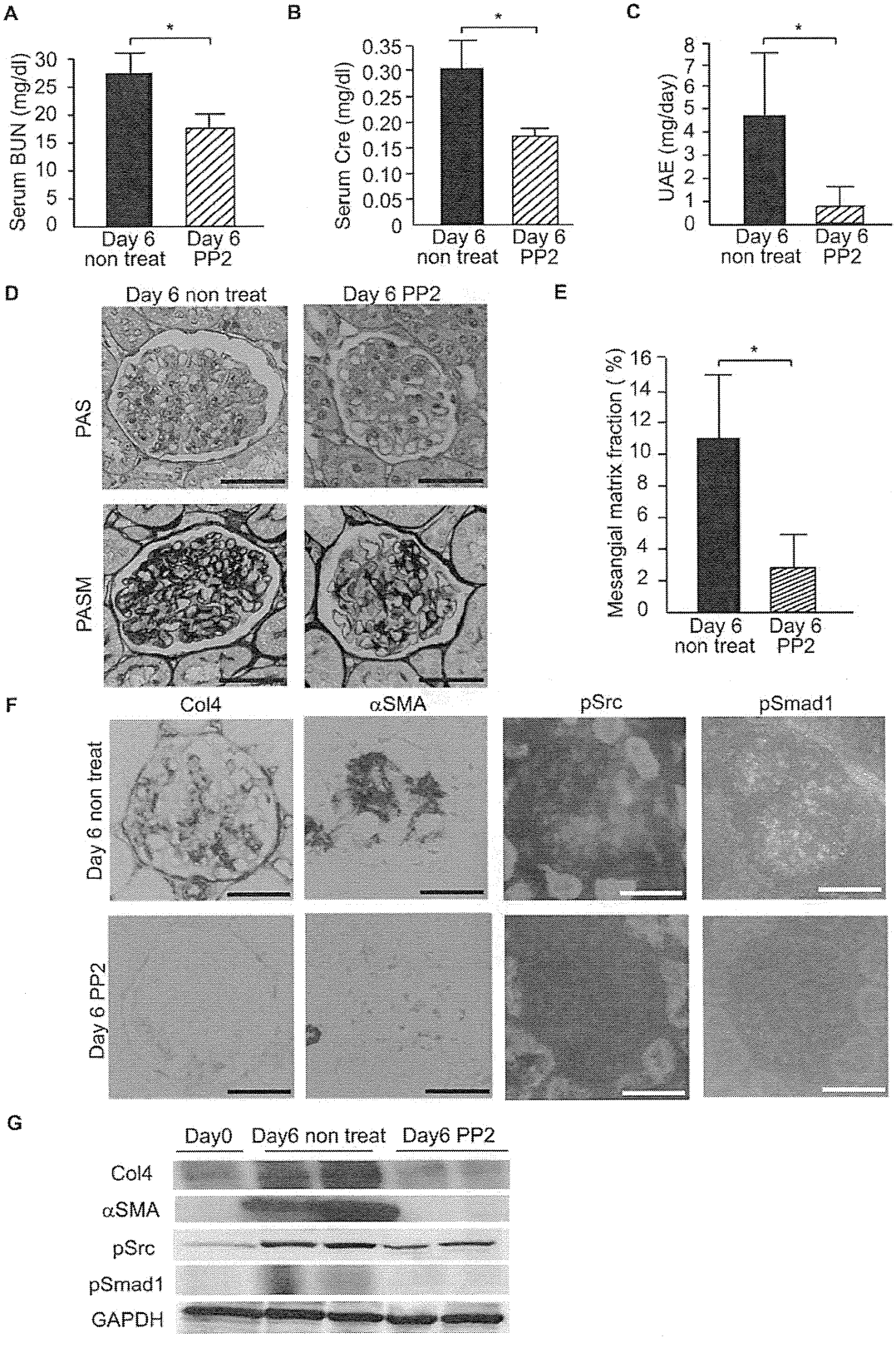

Figure 3. Src-specific inhibitor PP2 inhibits glomerulosclerosis and glomerular expression of pSrc and pSmad1 in Thy1 GN. (A–C) Serum blood urine nitrogen (BUN), serum creatinine (Cre), and UAE in the nontreatment and PP2 groups. *P* values were 0.001, 0.001 and 0.017, respectively. (D, E) Representative light-microscopic appearance of glomeruli (PAS and PASM staining) and quantitative assessment of PASM staining in Thy1 GN with or without PP2 on day 6. Scale bars = 100 μm. *$P<0.001$. (F) Immunohistochemistry of glomeruli (Col4, SMA, pSrc and pSmad1) in Thy1 GN with or without PP2 on day 6. Scale bars = 100 μm; n = 6 for each experimental group. (G) Western blot for the glomerular lysates from each group. Data represent mean values ± S.D. of at least three independent experiments; n = 6 for each experimental group on day 6.
doi:10.1371/journal.pone.0017929.g003

(Figure 4A–D). These results indicate that PDGF induced the expression of Col4 through the activation of Src/Smad1 signal transduction.

Silencing of c-Src in MCs inhibits PDGF-mediated phosphorylation of Smad1 and synthesis of Col4

To further confirm the role of c-Src in PDGF-induced upregulation of Smad1 and Col4 expression, c-Src gene silencing by siRNA was performed. c-Src silencing suppressed the PDGF-induced phosphorylation of Smad1 and the synthesis of Col4. In contrast, GAPDH protein levels, used as a loading control, were not affected across the samples (Figure 4E–H). We confirmed the result of knockdown experiments with PDGF stimulation by using three c-Src siRNAs (Src siRNA-1, -2, and -3) (Figure S2). We showed the representative data from using Src siRNA-3 in Figure 4E–H. From these results, c-Src may be significantly involved in PDGF-mediated Col4 expression.

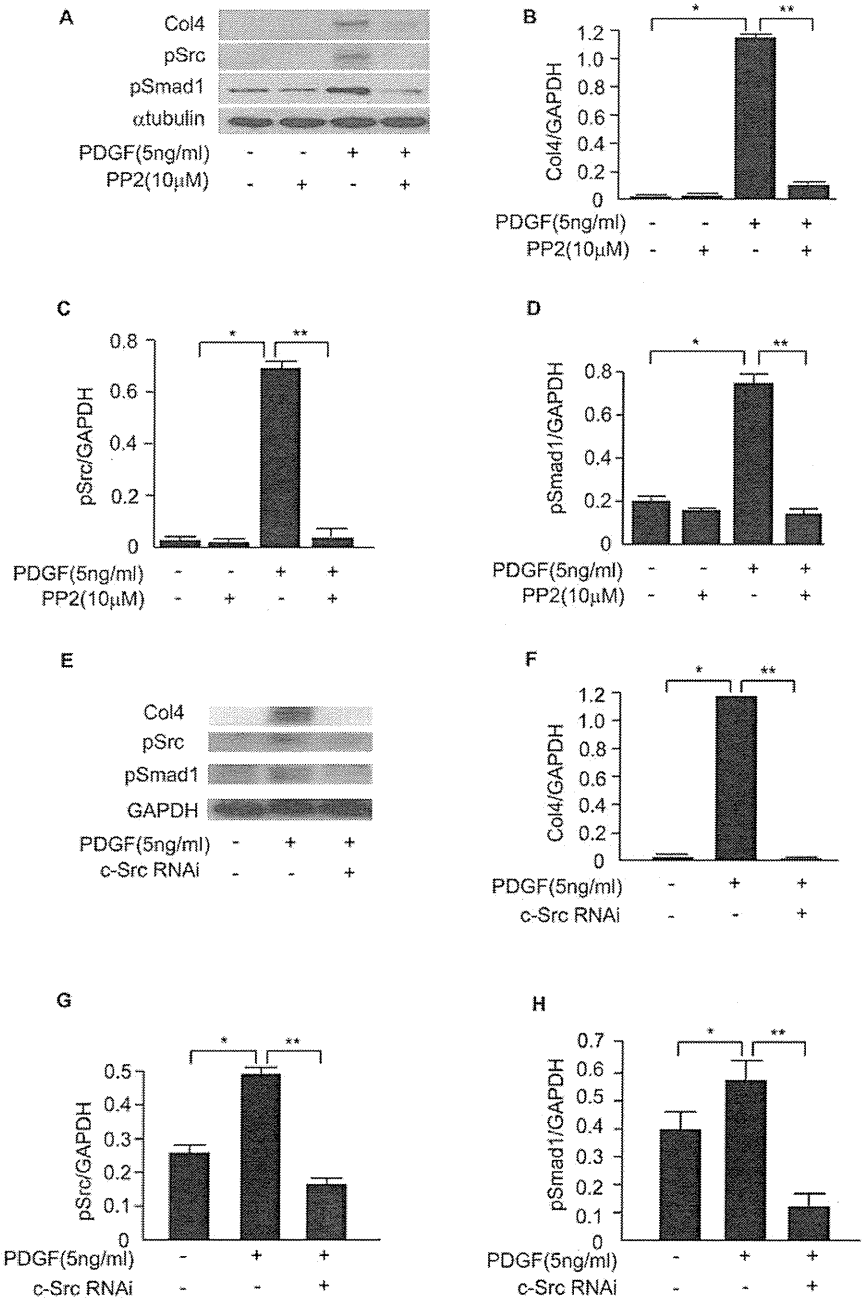

Figure 4. Activation of c-Src and Smad1 is regulated by PDGF in MCs. (A) Effect of PP2 on pSrc, pSmad1 and Col4. MCs were preincubated with PP2 (10 μM) or DMSO for 48 h before exposure to PDGF (5 ng/ml, 12 h). (B) Optical densitometry of Col4 in western blot. *$P<0.001$ and **$P<0.001$. (C, D) Optical densitometry of pSrc (*$P<0.001$ and **$P=0.003$) and pSmad1 (*$P=0.002$, **$P=0.002$) in western blot analyses. (E) Effects of RNAi-mediated silencing of c-Src on pSrc, pSmad1 and Col4 under stimulation of PDGF (5 ng/ml, 12 h). (F–H) Optical densitometry of Col4 (*$P<0.001$, **$P<0.001$), pSrc (*$P<0.001$, **$P<0.001$), and pSmad1 (*$P=0.02$, **$P=0.002$) in western blot. Data represent mean values ± S.D. of at least three independent experiments.

doi:10.1371/journal.pone.0017929.g004

Activated c-Src is associated with PDGFR in MCs

To clarify the intracellular interaction between PDGF signaling pathway and c-Src/Smad1 axis, the effects of constitutively active form of c-Src (caSrc) transfected in MCs was examined. Transient transfection of MCs with caSrc could induce phosphorylation of Smad1 wihtout stimulation of PDGF, and subsequently upregulated Col4 expression (Figure 5A). In contrast, transfection of the dominant negative Src (dnSrc) did not show these regulations. Moreover, we performed knockdown analysis using Smad1 siRNAs to confirm the role of Smad1 in the regulatory effect of PDGF-induced Col4 expression. Knockdown study revealed that Smad1 acts downstream of PDGF-c-Src signaling pathway in the induction of Col4 (Figure 5B). Furthermore we have explored the possibility that c-Src, while interacting directly with PDGF receptor, could transduce the PDGF signals in MCs. For this purpose, PDGF receptor was immunoprecipitated from whole cell lysates after PDGF stimulation. Anti-c-Src immunoblot revealed that c-Src really associates with PDGFR only when stimulated by PDGF (Figure 5C).

TGFβ signaling pathway partially mediated PDGF-induced Smad1/Col4 expression in MCs

Transforming growth factor beta (TGFβ) is an important growth factor in the modulation of cell proliferation as well as PDGF in a variety of cells. In addition, several studies reported that PDGF may increase the production of TGFβ and the expression of TGFβ type I receptor [25,26]. To elucidate the the molecular basis of the influence of PDGF on TGFβ signaling pathway, we performed TGFβ-neutralizing antibody assay for PDGF-stimulated MCs. PDGF increased the expressions of TGFβ and activin receptor-like kinase 5 (ALK5) and activated Smad1. However, these changes by PDGF could not be inhibited by neutralizing anti-TGFβ antibody (Figure 6A), indicating that PDGF, but not TGFβ, upregulates expression of ALK5, pSmad1, pSrc, and Col4. In particular, pSmad1 is phosphorylated by ALK1, but not by ALK5, therefore, we investigated the effects of high concentration of PDGF on MCs. At concentration of 50 ng/ml, PDGF increased the expressions of ALK1 as well as other proteins (Figure 6B). Interestingly, an addition of neutralizing anti-TGFβ antibody suppressed not only ALK1 expression, but also expressions of pSmad1 and Col4 (Figure 6B). These results suggest that PDGF has the potential to enhance TGFβ signal transduction through ALK1 as well as ALK5.

TGFβ signaling pathway partially mediated PDGF-induced Smad1/Col4 expression in MCs

To further elucidate the regulatory mechanisms controlling the cross-talk between PDGF and TGFβ in the activation of Smad1

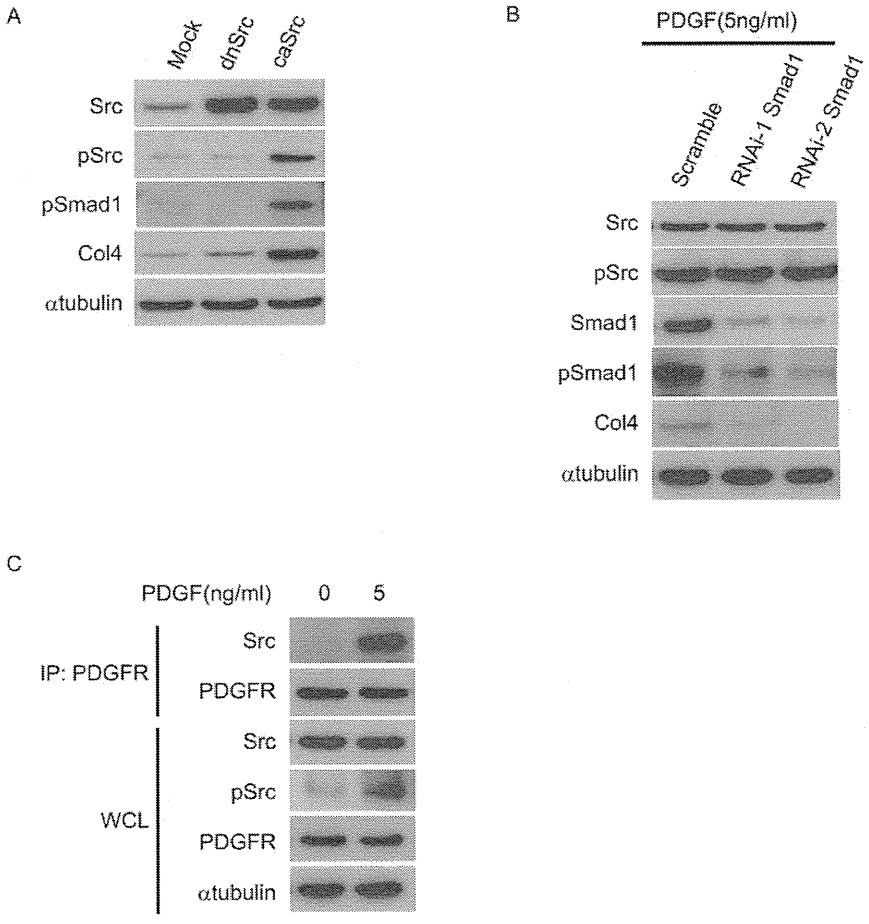

Figure 5. Activated c-Src is associated with PDGF Receptor (PDGFR) in MCs. (A) Western blot analyses of MCs transfected with constitutively active c-Src (caSrc), dominant negative c-Src (dnSrc), and empty vector (Mock). One of three independent experiments is shown. (B) Effects of RNAi-mediated silencing of Smad1 on pSmad1 and Col4 after 5 h stimulation of PDGF (5 ng/ml). Scrambled siRNA (Scramble) was used as a control. One of three independent experiments is shown. (C) MCs were serum-starved for 10 h and then incubated with 5 ng/ml of PDGF for 5 min. Whole cell lysates (WCL) were immunoprecipitated with polyclonal anti-PDGFR antibody and subjected to anti-Src immunoblot.
doi:10.1371/journal.pone.0017929.g005

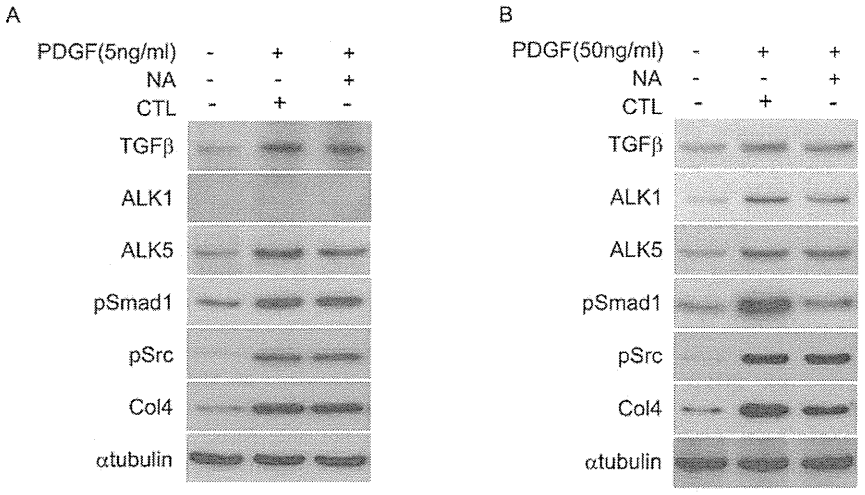

Figure 6. PDGF modulated TGFβ-Activin Receptor-like Kinases (ALKs) signaling pathways in MCs. (A, B) MCs were treated with neutralizing antibody for TGFβ (10 μg/ml) (NA) or control normal IgY (CTL) for 24 h prior to treatment with PDGF at indicated concentrations for 24 h. Equal amounts of cell lysates were subjected to Western blot. One of three independent experiments is shown.
doi:10.1371/journal.pone.0017929.g006

and induction of Col4 in MCs, we examined whether LDL receptor related protein-1 (LRP1) is involved in the signal pathways. Because Boucher et al. reported that LRP1 is tightly involved in the pathogenesis of atherosclerosis by regulating signaling of TGFβ and PDGF, and their receptors [27,28], knockdown analysis using LRP1 siRNAs was perfomed to examine the role of LRP1 in the regulatory effect of PDGF-induced Col4 expression and PDGF-activated TGFβ signaling pathway in MCs. Knockdown of LRP1 enhanced the downstream pathway of PDGF (Figure 7A) with the exception of ALK1 (Figure 7B). These results suggest that LRP1 has a significant inhibitory effect on PDGF signaling pathway leading to production of Col4 in MCs.

PDGF signaling pathway is partially involved in the AngII-induced c-Src/Smad1 signal activation in MCs

We previously reported that AngII activates the c-Src/Smad1 signaling pathway in the development of diabetic nephropathy and cultured MCs [23]. To investigate whether AngII signals influence the regulatory mechanisms of PDGF-induced c-Src/Smad1 signal transduction, we examined the inhibitory effects of APB5 and AngII receptor blocker (ARB) on the activation of c-Src, Smad1, and Col4 by AngII and PDGF, respectively. APB5 clearly attenuated the AngII-induced c-Src/Smad1/Col4 signal (Figure 8A). In contrast, ARB treatment slightly reduced PDGF-induced activation of the signal (Figure 8B). These data suggest that PDGF signaling pathway is activated by AngII in MCs.

Discussion

Cellular proliferation and extracellular matrix accumulation are characteristic features of progressive glomerular diseases, a major cause of end-stage renal failure in humans throughout much of the world. Glomerulosclerosis followed by mesangial proliferative glomerulonephritis is characterized by mesangial matrix expansion

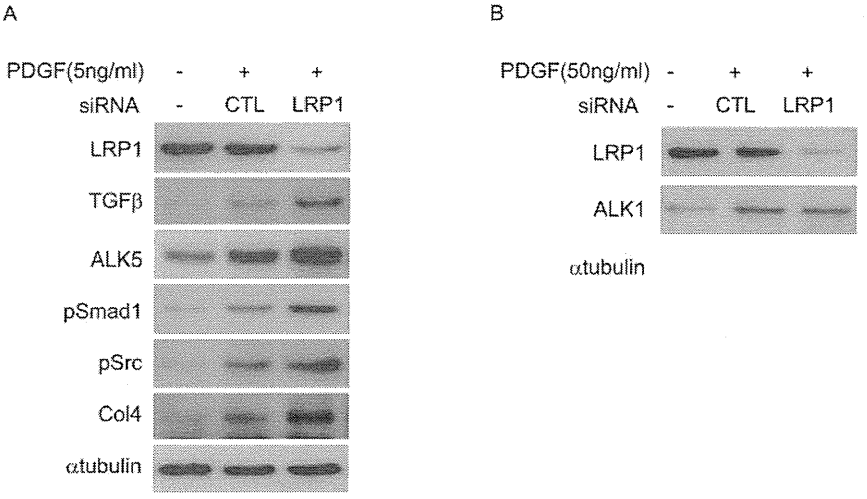

Figure 7. LRP1 modulated both PDGF and TGFβ signaling pathways in MCs. (A, B) Effects of PDGF stimulation and RNAi-mediated silencing of LRP1 after 5 h stimulation of PDGF at indicated concentrations on MCs. Scrambled siRNA (Scramble) was used as a control (CTL). Equal amounts of cell lysates were subjected to Western blot. One of three independent experiments is shown.
doi:10.1371/journal.pone.0017929.g007

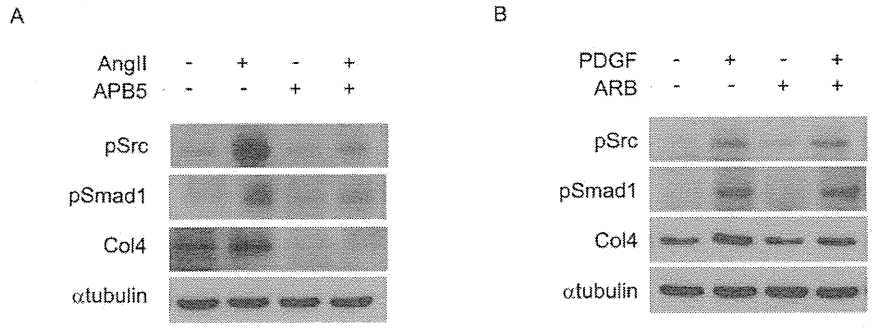

Figure 8. Molecular cross-talk between PDGF and AngII signaling pathways in MCs. (A) Effects of APB5 on pSrc, pSmad1 and Col4. MCs were preincubated with APB5 (100 ng/ml) or control rat IgG for 24 h before exposure to AngII (0.1 μM, 30 min). (B) Effects of olmesartan (ARB) on pSrc, pSmad1 and Col4. MCs were preincubated with olmesartan (10 μM) or methanol for 48 h before exposure to PDGF (5 ng/ml, 12 h). Equal amounts of cell lysates were subjected to Western blot. One of three independent experiments is shown.
doi:10.1371/journal.pone.0017929.g008

and phenotypic change of MCs [3]. In the expanded mesangial matrix, Col4 is a major component of ECM and is overproduced in glomerulosclerosis [6]. In addition, phenotypic modulation is a commonly observed feature in the progression of many renal diseases leading to CKD and ESRD. Expression of SMA is a well-known marker for the activation of MCs in most glomerular diseases. We previously reported that Smad1 upregulated the expression of Col4 and SMA [5,6] and thereby participates in the development of glomerulosclerosis in experimental glomerulonephritis [4]. However, the molecule that activates Smad1 in glomerulonephritis has not been fully elucidated. Since PDGF has been consistently implicated in cell proliferation and extracellular matrix accumulation, which characterize progressive glomerular disease [29], and since c-Src is an important component of the PDGF signaling pathway [30], we first investigated whether c-Src is induced in glomeruli of proliferative glomerulonephritis. In Thy1 GN, Col4 is strongly expressed in the sclerotic lesions of glomeruli, as previously described [4,21]. We show here that c-Src and Smad1 are heavily phosphorylated in the nuclei of glomerular cells in Thy1 GN. This phosphorylation parallels the progress of glomerulosclerosis and peaks on day 6, when Col4 and SMA expression levels have peaked. These results suggest that c-Src has a potential to be involved in the development of glomerulosclerosis in mesangial proliferative glomerulonephritis.

c-Src was identified as the first proto-oncogene, and a great deal of work has been carried out to elucidate its role in biological systems [31–33]. The two main areas in which Src inhibitors have been applied are regulating bone resorption [34,35] and both tumor growth and metastasis [36,37]. Most previous studies have shown that the role of Src family members is related to inflammatory responses. Additionally, the small chemical inhibitors that effectively and specifically block Src kinases could have great clinical implications for diseases with acute inflammatory responses [38,39]. In a rat renal ischemia-reperfusion injury model, increased active Src expression was found in the injured rat kidney after reperfusion [40]. To our knowledge, however, no report has demonstrated that c-Src is involved in the development of glomerulosclerosis in glomerular diseases. In the rat proliferative glomerulonephritis model, administration of PP2 completely abolished the phosphorylation of c-Src and Smad1 and resulted in the amelioration of glomerulosclerosis. Therefore, the activation of c-Src signal transduction plays a pivotal role in glomerulosclerosis, implicating it as a novel target of the therapeutic strategies for glomerulonephritis. Moreover, our findings show a new side of PP2 as an anti-glomerular disease agent.

In addition, PDGF is known to contribute to the development of both experimental and human glomerulonephritis [12,13]. Src kinase activation has been reported to contribute to PDGF-dependent cell-cycle proliferation, mitogenesis, and chemotaxis [24,29,30]. Thus, to investigate the molecular mechanisms underlying the progression of proliferative glomerulonephritis, we used cultured MCs under PDGF stimulation. PDGF induced phosphorylation of c-Src and Smad1 as well as Col4 expression, and these changes were blocked by PP2. The interaction between PDGFR and c-Src may be important for the phosphorylation of c-Src. In addition, the siRNA silencing experiments confirmed that c-Src regulated Smad1 activation. These findings suggest that c-Src activation is a key event in the PDGF-induced phosphorylation of Smad1, followed by the subsequent overproduction of Col4 in proliferative glomerulonephritis. In addition, PDGF activated TGFβ signaling pathways by induction of TGFβ and its type I receptors, ALK1 and ALK5. In particular, the induction of ALK1 may be an important event, because ALK1 transduce TGFβ signals to Smad1. Furthermore, several recent reports demonstrated that LRP1 has an inhibitory effect on TGFβ signaling pathway as well as PDGF signaling pathway [27,28]. As expected, LRP1 silencing exhibited additional effect on the activation of TGFβ signals by PDGF. Hence, LRP1 represents a promising new therapeutic target for the control of proliferative glomerular diseases. Moreover, our previous study demonstrated that AngII stimulated this Src-Smad1 axis independent of p44/42 MAP kinase activation and that the AngII receptor blocker ARB blocked this pathway. Because it is generally accepted that the AngII blockade significantly delays the progression of proliferative glomerulonephritis [41,42], our previous findings implied that the inhibition of the Src-Smad1 axis may partially explain the AngII-induced progression of proliferative glomerunonephritis. PDGF-induced activation of c-Src/Smad1 signaling pathway leading to Col4 production also plays an important role downstream of AngII stimulation, whereas ARB treatment did not fully suppressed the effect of PDGF. Chemical inhibitors directly or indirectly targeting Src kinases have been developed as potential drugs for the treatment of cancer [43]. It was recently reported that the inhibition of c-Src by these chemical inhibitors helps to prevent ischemia-reperfusion-induced injury in organs [38,39]. The present study raises the possibility that using these chemical inhibitors to block Src signal transduction could be a promising option for ameliorating proliferative glomerulonephritis as well as for the already reported effects of these inhibitors on excessive inflammatory cells, monocytes and macrophages [44,45]. Another report by Severgnini et al. demonstrated that c-Src controls

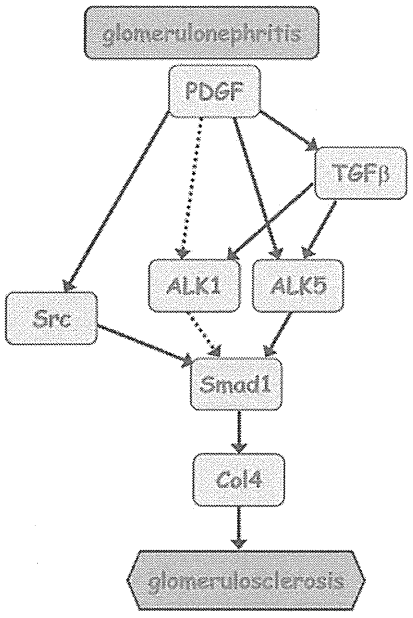

Figure 9. Proposed model for PDGF effects on Smad1 activation and Col4 expression in glomerulonephritis. Activation of Smad1 by PDGF mediates at least two different signal transduction pathways, TGFβ-ALK5-Smad1 and Src-Smad1. ALK1 may potentially activate Smad1 when exposed to high concentration of PDGF (broken arrows). The expression of ALK5 is induced by PDGF and is largely independent of TGFβ. Excessive activation of these signaling pathways may result in Col4 overproduction leading to the development of glomerulosclerosis in glomerulonephritis.
doi:10.1371/journal.pone.0017929.g009

STAT3 activation in acute lung injury [46]. In addition, we previously reported that STAT3 is involved in the development of glomerulosclerosis in experimental proliferative glomerulonephritis [4]. In light of these previous findings, our results highlight the importance of c-Src in the development of glomerulosclerosis in glomerulonephritis. Combining with our overall findings summarized in Figure 9, we can speculate that Smad1-mediated production of Col4 leading to mesangial expansion is a critical event in the development of glomerulosclerosis.

In conclusion, our present study indicates that c-Src activates Smad1-induced ECM production and phenotypic alteration, and is involving in the progression of proliferative glomerulonephritis leading to glomerulosclerosis. Further understanding of the Src/Smad1 pathway and the molecules involve in this pathway is critical for the clarification of glomerulosclerosis and to pave the way for a strategy to treat progressive glomerulonephritis.

Supporting Information

Figure S1 Time course of renal function in Thy1 GN. Urine volume (*P = 0.042) (A), serum BUN (*P = 0.014) (B), and UAE (*P = 0.017) (C) in Thy1 GN. Data represent mean values ± S.D. of at least three independent experiments; n = 6 for each experimental group.
(TIF)

Figure S2 Knockdown of c-Src expression. MCs were transfected with three different siRNAs specific for c-Src and with scrambled siRNA with or without PDGF stimulation. Effects of RNAi-mediated silencing of c-Src on pSrc, pSmad1 and Col4 under stimulation of PDGF (5 ng/ml, 12 h) were analyzed by Western blot. GAPDH served as a loading control.
(TIF)

Acknowledgments

We thank Hideo Uchiyama (Taigenkai Hospital), Maki Watanabe, Takako Pezzotti, Ayumi Hosotani (Kyoto University), and Akiko Sakurai (Tokushima University) for their excellent technical assistance. We are grateful to Dr. Nishikawa (RIKEN CDB) for providing APB5.

Author Contributions

Conceived and designed the experiments: TD H. Abe. Performed the experiments: AM H. Abe KN TM MA KT TT. Analyzed the data: H. Abe H. Arai NI AF TK TD. Wrote the paper: AM H. Abe.

References

1. Fogo A, Ichikawa I (1989) Evidence for a central role of glomerular growth in the development of sclerosis. Semin Nephrol 9: 329–342.
2. Striker LJ, Doi T, Elliot S, Striker GE (1989) The contribution of glomerular mesangial cells to progressive glomerulosclerosis. Semin Nephrol 9: 318–328.
3. Kagami S, Border WA, Miller DE, Noble NA (1994) Angiotensin II stimulates extracellular matrix protein synthesis through induction of transforming growth factor-beta expression in rat glomerular mesangial cells. J Clin Invest 93: 2431–2437.
4. Takahashi T, Abe H, Arai H, Matsubara T, Nagai K, et al. (2005) Activation of STAT3/Smad1 is a key signaling pathway for progression to glomerulosclerosis in experimental glomerulonephritis. J Biol Chem 280: 7100–7106.
5. Abe H, Matsubara T, Iehara N, Nagai K, Takahashi T, et al. (2004) Type IV collagen is transcriptionally regulated by Smad1 under advanced glycation end product (AGE) stimulation. J Biol Chem 279: 14201–14206.
6. Matsubara T, Abe H, Arai H, Nagai K, Mima A, et al. (2006) Expression of Smad1 is directly associated with mesangial matrix expansion in rat diabetic nephropathy. Lab Invest 86: 357–368.
7. Doi T, Vlassara H, Kirstein M, Yamada Y, Striker GE, et al. (1992) Receptor-specific increase in extracellular matrix production in mouse mesangial cells by advanced glycosylation end products is mediated via platelet-derived growth factor. Proc Natl Acad Sci USA 89: 2873–2877.
8. Tallquist M, Kazlauskas A (2004) PDGF signaling in cells and mice. Cytokine Growth Factor Rev 15: 205–213.
9. Leveen P, Pekny M, Gebre-Medhin S, Swolin B, Larsson E, et al. (1994) Mice deficient for PDGF B show renal, cardiovascular, and hematological abnormalities. Genes Dev 8: 1875–1887.
10. Lindahl P, Hellstrom M, Kalen M, Karlsson L, Pekny M, et al. (1998) Paracrine PDGF-B/PDGF-Rbeta signaling controls mesangial cell development in kidney glomeruli. Development 125: 3313–3322.
11. Soriano P (1994) Abnormal kidney development and hematological disorders in PDGF beta-receptor mutant mice. Genes Dev 8: 1888–1896.
12. Floege J, Eitner F, Alpers CE (2008) A new look at platelet-derived growth factor in renal disease. J Am Soc Nephrol 19: 12–23.
13. Johnson RJ, Floege J, Couser WG, Alpers CE (1993) Role of platelet-derived growth factor in glomerular disease. J Am Soc Nephrol 4: 119–128.
14. Johnson RJ, Raines EW, Floege J, Yoshimura A, Pritzl P, et al. (1992) Inhibition of mesangial cell proliferation and matrix expansion in glomerulonephritis in the rat by antibody to platelet-derived growth factor. J Exp Med 175: 1413–1416.
15. Brown MT, Cooper JA (1996) Regulation, substrates and functions of src. Biochim Biophys Acta 1287: 121–149.
16. Schlessinger J (2000) New roles for Src kinases in control of cell survival and angiogenesis. Cell 100: 293–296.
17. Waters CM, Connell MC, Pyne S, Pyne NJ (2005) c-Src is involved in regulating signal transmission from PDGFbeta receptor-GPCR(s) complexes in mammalian cells. Cell Signal 17: 263–277.
18. Silver BJ, Jaffer FE, Abboud HE (1989) Platelet-derived growth factor synthesis in mesangial cells: induction by multiple peptide mitogens. Proc Natl Acad Sci U S A 86: 1056–1060.
19. Floege J, Eng E, Young BA, Alpers CE, Barrett TB, et al. (1993) Infusion of platelet-derived growth factor or basic fibroblast growth factor induces selective glomerular mesangial cell proliferation and matrix accumulation in rats. J Clin Invest 92: 2952–2962.
20. MacKay K, Striker LJ, Elliot S, Pinkert CA, Brinster RL, et al. (1988) Glomerular epithelial, mesangial, and endothelial cell lines from transgenic mice. Kidney Int 33: 677–684.
21. Makibayashi K, Tatematsu M, Hirata M, Fukushima N, Kusano K, et al. (2001) A vitamin D analog ameliorates glomerular injury on rat glomerulonephritis. Am J Pathol 158: 1733–1741.

22. Mima A, Arai H, Matsubara T, Abe H, Nagai K, et al. (2008) Urinary Smad1 is a novel marker to predict later onset of mesangial matrix expansion in diabetic nephropathy. Diabetes 57: 1712–1722.
23. Mima A, Matsubara T, Arai H, Abe H, Nagai K, et al. (2006) Angiotensin II-dependent Src and Smad1 signaling pathway is crucial for the development of diabetic nephropathy. Lab Invest 86: 927–939.
24. Yamamoto Y, Kato I, Doi T, Yonekura H, Ohashi S, et al. (2001) Development and prevention of advanced diabetic nephropathy in RAGE-overexpressing mice. J Clin Invest 108: 261–268.
25. Throckmorton DC, Brogden AP, Min B, Rasmussen H, Kashgarian M (1995) PDGF and TGF-beta mediate collagen production by mesangial cells exposed to advanced glycosylation end products. Kidney Int 48: 111–117.
26. Pan D, Yang J, Lu F, Xu D, Zhou L, et al. (2007) Platelet-derived growth factor BB modulates PCNA protein synthesis partially through the transforming growth factor beta signalling pathway in vascular smooth muscle cells. Biochem Cell Biol 85: 606–615.
27. Boucher P, Gotthardt M, Li WP, Anderson RG, Herz J (2003) LRP: role in vascular wall integrity and protection from atherosclerosis Science 300: 329–332.
28. Boucher P, Li WP, Matz RL, Takayama Y, Auwerx J, et al. (2007) LRP1 functions as an atheroprotective integrator of TGFbeta and PDFG signals in the vascular wall: implications for Marfan syndrome. PLoS One 2: e448.
29. Floege J, Johnson RJ (1995) Multiple roles for platelet-derived growth factor in renal disease. Miner Electrolyte Metab 21: 271–282.
30. Kypta RM, Goldberg Y, Ulug ET, Courtneidge SA (1990) Association between the PDGF receptor and members of the src family of tyrosine kinases. Cell 62: 481–92.
31. Stehelin D, Varmus HE, Bishop JM, Vogt PK (1976) DNA related to the transforming gene(s) of avian sarcoma viruses is present in normal avian DNA. Nature 260: 170–173.
32. Golden A, Nemeth SP, Brugge JS (1986) Blood platelets express high levels of the pp60c-src-specific tyrosine kinase activity. Proc Natl Acad Sci USA 83: 852–856.
33. Soriano P, Montgomery C, Geske R, Bradley A (1991) Targeted disruption of the c-src proto-oncogene leads to osteopetrosis in mice. Cell 64: 693–702.
34. Lowe C, Yoneda T, Boyce BF, Chen H, Mundy GR, et al. (1993) Osteopetrosis in Src-deficient mice is due to an autonomous defect of osteoclasts. Proc Natl Acad Sci USA 90: 4485–4489.
35. Tanaka S, Amling M, Neff L, Peyman A, Uhlmann E, et al. (1996) c-Cbl is downstream of c-Src in a signalling pathway necessary for bone resorption. Nature 383: 528–531.
36. Trevino JG, Summy JM, Lesslie DP, Parikh NU, Hong DS, et al. (2006) Inhibition of SRC expression and activity inhibits tumor progression and metastasis of human pancreatic adenocarcinoma cells in an orthotopic nude mouse model. Am J Pathol 168: 962–972.
37. Mandal M, Myers JN, Lippman SM, Johnson FM, Williams MD, et al. (2008) Epithelial to mesenchymal transition in head and neck squamous carcinoma: association of Src activation with E-cadherin down-regulation, vimentin expression, and aggressive tumor features. Cancer 112: 2088–2100.
38. Severgnini M, Takahashi S, Tu P, Perides G, Homer RJ, et al. (2005) Inhibition of the Src and Jak kinases protects against lipopolysaccharide-induced acute lung injury. Am J Respir Crit Care Med 171: 858–867.
39. Okutani D, Lodyga M, Han B, Liu M (2006) Src protein tyrosine kinase family and acute inflammatory responses. Am J Physiol Lung Cell Mol Physiol 291: L129–141.
40. Takikita-Suzuki M, Haneda M, Sasahara M, Owada MK, Nakagawa T, et al. (2003) Activation of Src kinase in platelet-derived growth factor-B-dependent tubular regeneration after acute ischemic renal injury. Am J Pathol 163: 277–286.
41. Peters H, Border WA, Noble NA (1998) Targeting TGF-beta overexpression in renal disease: maximizing the antifibrotic action of angiotensin II blockade. Kidney Int 54: 1570–1580.
42. Catapano F, Chiodini P, De Nicola L, Minutolo R, Zamboli P, et al. (2008) Antiproteinuric response to dual blockade of the renin-angiotensin system in primary glomerulonephritis: meta-analysis and metaregression. Am J Kidney Dis 52: 475–485.
43. Spreafico A, Schenone S, Serchi T, Orlandini M, Angelucci A, et al. (2008) Antiproliferative and proapoptotic activities of new pyrazolo[3,4-d]pyrimidine derivative Src kinase inhibitors in human osteosarcoma cells. FASEB J 22: 1560–1571.
44. Huang WC, Chen JJ, Chen CC (2003) c-Src-dependent tyrosine phosphorylation of IKKbeta is involved in tumor necrosis factor-alpha-induced intercellular adhesion molecule-1 expression. J Biol Chem 278: 9944–9952.
45. Huang WC, Chen JJ, Inoue H, Chen CC (2003) Tyrosine phosphorylation of I-kappa B kinase alpha/beta by protein kinase C-dependent c-Src activation is involved in TNF-alpha-induced cyclooxygenase-2 expression. J Immunol 170: 4767–4775.
46. Severgnini M, Takahashi S, Rozo LM, Homer RJ, Kuhn C, et al. (2004) Activation of the STAT pathway in acute lung injury. Am J Physiol Lung Cell Mol Physiol 286: L1282–1292.

Atherosclerosis 214 (2011) 404–407

Contents lists available at ScienceDirect

Atherosclerosis

journal homepage: www.elsevier.com/locate/atherosclerosis

Molecular genetic epidemiology of homozygous familial hypercholesterolemia in the Hokuriku district of Japan

Hiroshi Mabuchi[a,*], Atsushi Nohara[a], Tohru Noguchi[a], Junji Kobayashi[a], Masa-aki Kawashiri[b], Hayato Tada[b], Chiaki Nakanishi[b], Mika Mori[b], Masakazu Yamagishi[b], Akihiro Inazu[c], Junji Koizumi[d], the Hokuriku FH Study Group

[a] Department of Lipidology, Graduate School of Medical Science, Kanazawa University, Japan
[b] Division of Cardiovascular Medicine, Graduate School of Medical Science, Kanazawa University, Japan
[c] Laboratory Science, Graduate School of Medical Science, Kanazawa University, Japan
[d] General Medicine, Graduate School of Medical Science, Kanazawa University, Japan

ARTICLE INFO

Article history:
Received 29 March 2010
Received in revised form 5 November 2010
Accepted 7 November 2010
Available online 13 November 2010

Keywords:
Familial hypercholesterolemia (FH)
DNA analysis of FH genes
Genetic epidemiology of homozygous FH
Incidence of FH

ABSTRACT

Aim: Familial hypercholesterolemia (FH) is caused by mutations of FH genes, i.e. LDL-receptor (LDLR), PCSK9 and apolipoprotein B (ApoB) gene. We evaluated the usefulness of DNA analysis for the diagnosis of homozygous FH (homo-FH), and studied the frequency of FH in the Hokuriku district of Japan.
Methods: Twenty-five homo-FH patients were recruited. LDLR mutations were identified using the Invader assay method. Mutations in PCSK9 were detected by PCR-SSCP followed by direct sequence analysis.
Results: We confirmed 15 true homozygotes and 10 compound heterozygotes for LDLR mutations. Three types of double heterozygotes for LDLR and PCSK9 were found. No FH patients due to ApoB mutations were found. The incidences of homo-FH and hetero-FH in the Hokuriku district were 1/171,167 and 1/208, respectively.
Conclusions: Our observations underlined the value of FH gene analysis in diagnosing homo-FH and confirmed extraordinarily high frequency of FH in the Hokuriku district of Japan.

1. Introduction

Familial hypercholesterolemia (FH) is an autosomal dominant disease characterized by the triad of (1) hypercholesterolemia due to a high level of plasma low-density-lipoprotein (LDL), (2) tendon xanthomas and (3) premature coronary heart disease [1]. Patients with homozygous FH (homo-FH) have two mutant alleles of either of three FH-associated genes (FH genes), which are as follows: LDL-receptor (LDLR), proprotein convertase subtilisin/kexin type 9 (PCSK9) and apolipoprotein B (ApoB) gene [2]. Homo-FH patients are likely to be identified in early childhood because of the early appearance of xanthomatosis associated with an exceptionally high plasma cholesterol levels (exceeding 15.6 mmol/l), reflecting an extreme increase in LDL concentration. Use of the classical diagnosis of homo-FH and hetero-FH has led to an estimate of the prevalence of homo- and hetero-FH is 1 in 1,000,000 and 1 in 500 persons, respectively throughout the world [1]. The clinical phenotype of FH is highly variable and depends on the FH genes mutations present. Patients with a mild phenotype of homozygous FH often show a heterozygous phenotype of FH. Our aims of the present study were two. First we evaluated the molecular genetic epidemiology of homo-FH and then studied the frequency of hetero- and homo-FH in the Hokuriku district of Japan.

2. Patients and methods

2.1. Diagnostic criteria of FH [3,4]

I. Hetero-FH
   a) Clinical diagnostic criteria are hypercholesterolemia with tendon xanthomas, or hypercholesterolemia in the first- or second-degree relative of FH patients.
   b) Genetic diagnostic criteria are mutations of FH genes.
II. Homo-FH
   a) Clinical diagnostic criteria are juvenile xanthomatosis with plasma cholesterol level about twice that of parents or other family members with hetero-FH.
   b) Genetic diagnostic criteria are true homozygotes, compound heterozygotes and double heterozygotes for FH genes.

* Corresponding author at: Department of Lipidology, Graduate School of Medical Science, Kanazawa University, Takara-machi 13-1, Kanazawa 920-8640, Japan. Tel.: +81 76 265 2265; fax: +81 76 234 4271.
E-mail address: mabuchi@med.kanazawa-u.ac.jp (H. Mabuchi).

0021-9150/$ – see front matter © 2010 Elsevier Ireland Ltd. All rights reserved.
doi:10.1016/j.atherosclerosis.2010.11.005

Table 1
Clinical characteristics of 25 homo-FH patients in Hokuriku district of Japan.

	Case no.	Family no.	Name	FH gene mutations	Sex	Age (years)	TC (mmol/L)	TG (mmol/L)	LDL-C (mmol/L)	HDL-C (mmol/L)	ATT (mm)	Father/mother	Consanguineous marriage	Outcome
True homozygote	1	1	M.K.	Ex2-3del/Ex2-3del	F	40	14.3	1.61	12.9	0.7	8	?/Hetero	+	D
	2	2	H.Y.	Ex2-3del/Ex2-3del	F	34	16.4	0.91	13.3	1.5	27	?/Hetero	+	A (LDL-a)
	3	3	T.T.	Ex2-3del/Ex2-3del	M	49	14.5	4.38				?/Hetero	+	D
	4	3	Y.I.	Ex2-3del/Ex2-3del	F	52	16.2	3.56	13.7	0.8	31	?/Hetero	+	A (med)
	5	4	M.I.	K790X/K790X	F	20	19.0	3.08				Hetero/hetero	?	D
	6	5	S.S.	K790X/K790X	F	26	26.1	8.85			20	Hetero/hetero	–	D
	7	5	Y.S.	K790X/K790X	F	23	13.9	1.11	12.9	0.5	20	Hetero/hetero	–	A (LDL-a)
	8	6	S.Y.	D280Y/D280Y	M	24	13.9	0.55	12.9	0.8	42	Hetero/hetero	+	A (LDL-a)
	9	6	K.Y.	D280Y/D280Y	F	27	15.8	1.42			13	Hetero/hetero	+	D
	10	6	K.M.	D280Y/D280Y	F	40	15.9	2.03			25	Hetero/hetero	+	D
	11	7	M.N.	R395W/R395W	F	73	15.6	1.21	14.4	0.6	11	?/?	?	D
	12	8	A.Y.	V502M/V502M	M	28	13.0	1.30			17	Hetero/hetero	–	A (med)
	13	9	Y.E.	IVS15-3C>A/IVS15-3C>A	M	11	23.6	3.39				Hetero/hetero	–	D
	14	10	S.Y.	PCSK9 E32K/PCSK9 E32K	F	49	10.9	1.73	8.2	1.3	9	?/?	?	A (med)
	15	11	Y.G.	PCSK9 E32K/PCSK9 E32K	F	44	8.4	1.95	6.1	1.4		Hetero/hetero	–	A (med)
Compound heterozygote	16	13	A.T.	K790X/P664L	M	5	17.8	3.05	15.1	0.7	6	Hetero/hetero	–	A (LDL-a)
	17	13	M.T.	K790X/P664L	M	15	14.1	2.73	11.4	0.8	9	Hetero/hetero	–	A (LDL-a)
	18	14	N.Y.	K790X/?	F	36	11.1	1.05	9.5	1.0	14	Hetero/hetero	–	A (med)
	19	15	K.C.	C163R/?	F	21	12.8	0.80	11.1	1.4	10	Hetero/hetero	–	A (med)
	20	16	Y.T.	Exon3-6dup/?	M	48	15.1	8.67		0.8	30	?/?	?	A (med)
	21	17	M.M.	W23X/?	M	36	12.0	2.42	9.8	1.0	28	Hetero/hetero	–	A (LDL-a)
	22	18	H.T.	R94H/W159X	M	59	12.8	1.45	11.1	1.0	22	?/?	–	A (med)
	23	19	Y.G.	IVS15-3C>A/PCSK9 E32K	M	45	12.0	2.51	9.6	1.3	15	?/hetero	–	A (med)
	24	20	T.K.	K790X/PCSK9 E32K	M	1	9.0	2.55	6.4	1.4	–	Hetero/hetero	–	A (med)
	25	21	M.K.	C183S/PCSK9E32K	M	3	16.4	1.25	14.2	0.7	-	Hetero/hetero	–	A (med)

Data are shown in mmol/L; F: female, M: male; ATT: achilles tendon thickness; Hetero: hetero-FH; D; deceased; A; alive; LDL-a: LDL-apheresis; med: medication.

2.2. Patients

Twenty-five clinically or genetically diagnosed homo-FH patients were selected for the study of genetic epidemiology of homo-FH and the calculation of the incidence of FH in the Hokuriku district. Written informed consent was obtained from each of the subjects prior to participation in the study.

2.3. Laboratory measurements

Blood samples for assays were drawn after overnight fasting. Concentrations of plasma total cholesterol (TC), triglyceride (TG) and high-density-lipoprotein-cholesterol (HDL-C) were determined at accredited clinical laboratories using routine clinical methods. LDL-cholesterol (LDL-C) concentrations were calculated using the Friedewald equation [5].

2.4. FH genes analysis

Detailed methods of FH genes analysis were described in our previous paper [6], and are described in brief here. Genomic DNA was prepared from white blood cells using a Genomic DNA Purification Kit (Gentra Systems, Minneapolis, MN, USA). Primers covering all of the exons and exon–intron boundary sequence of LDLR and PCSK9 were designed using Primer3 online software (http://frodo.wi.mit.edu/). LDLR mutations were identified using the Invader assay method (Third Wave Technologies, Inc., Madison, WI, USA) for point mutations previously identified in Japan [7]. The multiplex ligation-dependent probe amplification (MLPA) method for large rearrangements was performed using a P062B LDLR MLPA kit (MRC Holland, Amsterdam, Netherlands) and DNA sequencing was performed using a BigDye Terminator v3.1 Cycle Sequencing Kit (Applied Biosystems, Foster City, CA, USA) for the other mutations. ApoB mutations were screened by the methods reported in our previous paper [8]. Mutations in PCSK9 were detected by polymerase chain reaction (PCR) single-strand conformational polymorphism (SSCP) followed by direct sequence analysis.

2.5. Statistical analysis

Plasma lipid concentrations were compared among FH groups using Student's *t*-test. All data in the text are expressed as mean ± SD. JMP 5.1.2 software (SAS Institute, Cary, NC, USA) was used for statistical analyses. $p < 0.05$ was considered statistically significant.

3. Results

3.1. Genotypic analyses of homo-FH patients

A DNA study of FH gene mutations was performed in all 25 clinically and genetically diagnosed homo-FH patients. Thirteen LDL-R mutants were found in these homo-FH patients, and one PCSK9 mutant (PCSK9 E32K) was found in five patients (Table 1). True homo-FH was confirmed in 15 patients (Table 1, Fig. 1), and six true homozygotes (13 patients) were for LDLR mutations, and one (2 patients) was true homozygote for PCSK9 E32K. Four true homozygotes of Ex2-3del in three families and three homozygotes of D280Y in one family were born to consanguineous marriage. The geographical distributions of these homo-FH patients are shown in Fig. 1. Nine types of compound LDLR mutations were found in 10 homo-FH patients. Three types of LDLR and PCSK9 double heterozygotes were found. No case of FH patients due to ApoB mutation was

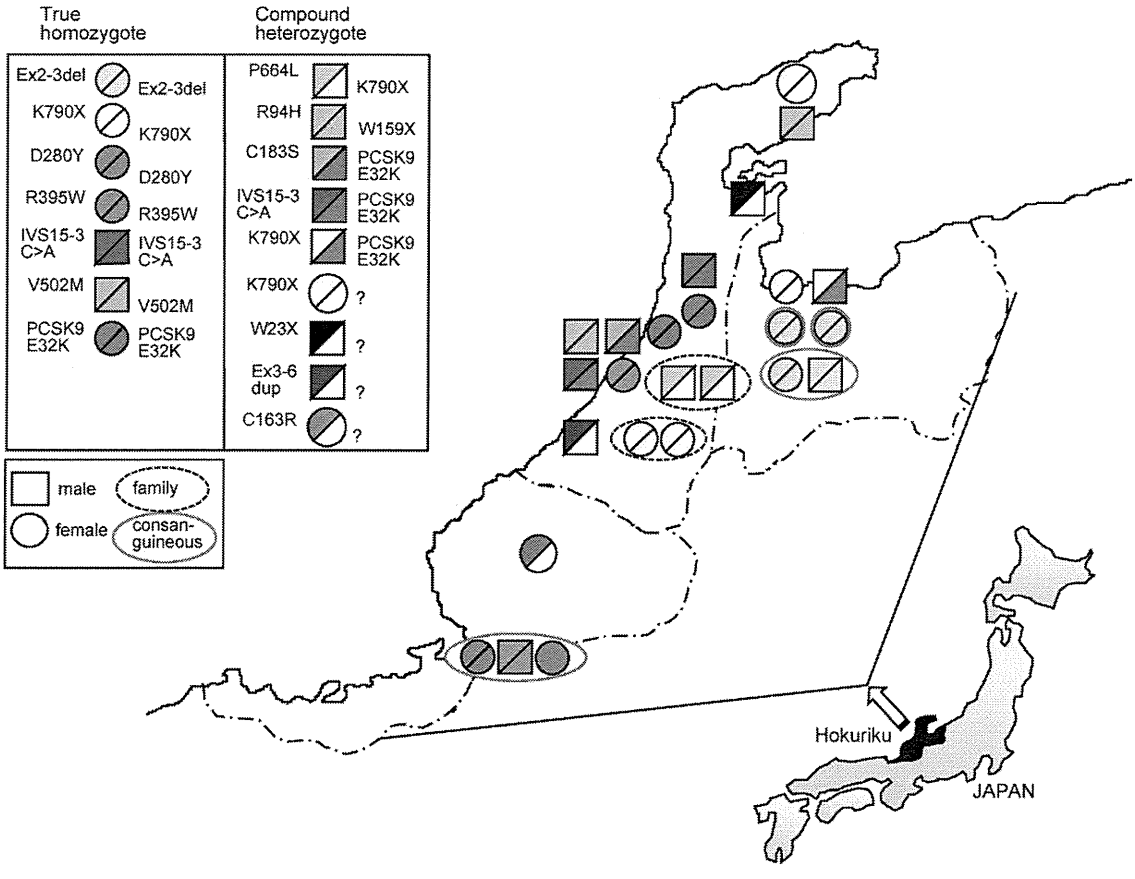

Fig. 1. Geographical location of 25 homo-FH patients with FH gene mutations in the Hokuriku district of Japan.

found. No consanguineous marriage was found in these compound or double heterozygote families (Table 1, Fig. 1).

Thirteen cases diagnosed by DNA analysis showed less than 14.3 mmol/L of TC. Mean (±SD) TC levels (15.7 ± 4.0 mmol/L) in homo-FH patients confirmed by DNA analysis were significantly lower than those (18.5 ± 4.1 mmol/L) diagnosed by clinical criteria ($p < 0.0442$) [9]. Two patients who were true homozygotes due to a mutation in the PCSK9 gene were newly found among our homozygotes. PCSK9 E32K produced relatively mild homo-FH phenotypes. The mean (±SD) plasma cholesterol level in homozygotes for LDLR gene mutations (15.7 ± 3.8 mmol/L) was significantly higher than that (11.3 ± 3.2 mmol/L) in true homozygotes or double heterozygotes for PCSK9 mutations ($p < 0.0276$).

The outcomes of the patients are shown in Table 1. Seven patients died of cardiac death and one (M.K.) died of leukemia. Seventeen patients are alive, and 6 patients have been treated with LDL-apheresis, and 11 patients with medications (Table 1).

3.2. Frequency of FH calculated using the Hardy–Weinberg equilibrium

Among 11 true homo-FH families consanguineous marriage was detected in four. In the remaining seven families, there were no consanguineous marriages. In nine families of compound heterozygotes no consanguineous marriage was found (Table 1, Fig. 1). The Hardy–Weinberg equilibrium was used to calculate the frequency of hetero-FH. The frequencies of homo-FH, hetero-FH and unaffected persons are p^2, $2pq$ and q^2, respectively (where $p+q=1$) and the general population in the Hokuriku district was 3,081,000. If the 7 patients from consanguineous marriage were ignored, p^2 could be 18/3,081,000 = 1/171,167 and then $p = 1/414$. As $q = 1 - p = 413/414$, the frequency of the hetero-FH ($2pq$) is $2 \times 1/414 \times 413/414 = 1/208$. Therefore, frequencies of the homo-FH and the hetero-FH were 1/171,167 and 1/208, respectively.

4. Discussion

It has been thought that homo-FH is easily diagnosed. However, it is sometimes difficult to differentiate severely affected heterozygotes from mild-type homozygotes without DNA analysis of FH genes. Recently, analysis of FH gene mutations has made it possible to identify presymptomatic homo-FH phenotype. DNA analysis of FH-associated genes shows true homozygote of identical heterozygous mutant, compound heterozygote of different heterozygous mutant of the same gene, and double heterozygote of different FH gene mutations. True homozygotes often came from a consanguineous marriage, whereas compound or double heterozygotes almost never did so. True homozygotes and compound heterozygotes for PCSK9 E32K show mild phenotypic homo-FH, compared with LDLR mutant homo-FH patients [6]. Currently, the diagnosis of FH involves clinical assessment and biochemical tests (lipid profile), but DNA-based testing will play a greater role in the identification and management of FH [10].

The prevalence of hetero-FH among the general population has been estimated to be at least, 1 in 500 among Caucasians, ranging from 1 in 200 to 1 in 1000 [11,12]. In 1978, we summarized 51 homozygous patients with FH in Japan, and estimated the frequency of homo-FH in Japan as 1 in 1.45 millions, and that of hetero-FH as 1 in 500 [9]. However, the low incidence of FH in most countries is due to the low frequency of homo-FH diagnosed by classical diagnostic criteria based on physical signs, laboratory findings and data from the parents. In the present study genetic diagnosis detected unexpectedly mild phenotypic cases of homo-FH, and several new cases of homo-FH were discovered. As FH is an autosomal dominant genetic disease, the frequency of hetero-FH has been calculated by the incidence of homo-FH in the district using the Hardy–Weinberg equilibrium. Here we found an extraordinarily high incidence of FH in this district of Japan.

A remarkably high prevalence of FH has been reported in several areas of the world, owing to founder effects. In Lebanon, the estimated prevalence of homozygotes and heterozygotes is 1 in 10,000 and 1 in 171, respectively [13]. In the Hokuriku district of Japan, the most frequent mutation in hetero-FH was the K790X LDLR mutation, with a frequency of 31.7% [7]. However, this mutant was less frequent in the Osaka district (5.4%) in Japan. No historical immigration records have been maintained in this district, and thus the K790X mutant of LDLR should not be classified as a founder gene in Japan, but only as a historically old mutant that prevailed locally and widely over a long period of time. High frequency of FH gene mutations might have produced true homozygotes without consanguineous marriage.

These observations underline the value of gene analysis in diagnosing hetero- and homo-FH patients and the extraordinarily high frequency of FH in this district of Japan.

Conflict of interest

There is no conflict of interest to disclosure.

References

[1] Goldstein JL, Hobbs HH, Brown MS. Familial hypercholesterolemia. In: Scriver C, Beaudet A, Sly W, Valle D, Childs B, Kinzler K, Vogelstein B, editors. The metabolic and molecular bases of inherited disease. 8th ed. McGraw-Hill Professional; 2000. p. 2895.
[2] Soutar AK, Naoumova RP. Mechanisms of disease: genetic causes of familial hypercholesterolemia. Nat Clin Pract Cardiovasc Med 2007;4(4):214–25.
[3] Mabuchi H, Higashikata T, Nohara A, et al. Cutoff point separating affected and unaffected familial hypercholesterolemic patients validated by LDL-receptor gene mutants. J Atheroscler Thromb 2005;12(1):35–40.
[4] Scientific Steering Committee on behalf of the Simon Broome Register Group. Risk of fatal coronary heart disease in familial hypercholesterolaemia. BMJ 1991;303(6807):893–6.
[5] Friedewald WT, Levy RI, Fredrickson DS. Estimation of the concentration of low-density lipoprotein cholesterol in plasma, without use of the preparative ultracentrifuge. Clin Chem 1972;18(6):499–502.
[6] Noguchi T, Katsuda S, Kawashiri MA, et al. The E32K variant of PCSK9 exacerbates the phenotype of familial hypercholesterolemia by increasing PCSK9 function and concentration in the circulation. Atherosclerosis 2010;210(1):166–72.
[7] Yu W, Nohara A, Higashikata T, et al. Molecular genetic analysis of familial hypercholesterolemia: spectrum and regional difference of LDL receptor gene mutations in Japanese population. Atherosclerosis 2002;165(2):335–42.
[8] Nohara A, Yagi K, Inazu A, et al. Absence of familial defective apolipoprotein B-100 in Japanese patients with familial hypercholesterolaemia. Lancet 1995;345(8962):1438.
[9] Mabuchi H, Tatami R, Haba T, et al. Homozygous familial hypercholesterolemia in Japan. Am J Med 1978;65(2):290–7.
[10] Kolansky DM, Cuchel M, Clark BJ, et al. Longitudinal evaluation and assessment of cardiovascular disease in patients with homozygous familial hypercholesterolemia. Am J Cardiol 2008;102(11):1438–43.
[11] Goldstein JL, Schrott HG, Hazzard WR, et al. Hyperlipidemia in coronary heart disease. II. Genetic analysis of lipid levels in 176 families and delineation of a new inherited disorder, combined hyperlipidemia. J Clin Invest 1973;52(7):1544–68.
[12] Slack J. Inheritance of familial hypercholesterolemia. Atheroscler Rev 1979;5:35–66.
[13] Khachadurian AK. The inheritance of essential familial hypercholesterolemia. Am J Med 1964;37:402–7.

Atherosclerosis 217 (2011) 165–170

Contents lists available at ScienceDirect

Atherosclerosis

journal homepage: www.elsevier.com/locate/atherosclerosis

Comparison of effects of bezafibrate and fenofibrate on circulating proprotein convertase subtilisin/kexin type 9 and adipocytokine levels in dyslipidemic subjects with impaired glucose tolerance or type 2 diabetes mellitus: Results from a crossover study

Tohru Noguchi[a], Junji Kobayashi[a,*], Kunimasa Yagi[b], Atsushi Nohara[a], Naoto Yamaaki[b], Masako Sugihara[b], Naoko Ito[b], Rie Oka[c], Masa-aki Kawashiri[b], Hayato Tada[b], Mutsuko Takata[b], Akihiro Inazu[d], Masakazu Yamagishi[b], Hiroshi Mabuchi[a]

[a] *Department of Lipidology, Graduate School of Medical Science, Kanazawa University, Takara-machi 13-1, Kanazawa 920-8640, Japan*
[b] *Division of Cardiovascular Medicine, Graduate School of Medical Science, Kanazawa University, Japan*
[c] *Department of Internal Medicine, Hokuriku Chuo Hospital, Japan*
[d] *Laboratory Science, Graduate School of Medical Science, Kanazawa University, Japan*

ARTICLE INFO

Article history:
Received 10 November 2010
Received in revised form 17 January 2011
Accepted 7 February 2011
Available online 22 February 2011

Keywords:
PCSK9
Bezafibrate
Fenofibrate
Diabetes
Dyslipidemia
Peroxisome proliferator-activated receptor (PPAR)
Adiponectin

ABSTRACT

Background: Bezafibrate and fenofibrate show different binding properties against peroxisome proliferator-activated receptor subtypes, which could cause different clinical effects on circulating proprotein convertase subtilisin/kexin type 9 (PCSK9) levels and on various metabolic markers.
Methods: An open, randomized, four-phased crossover study using 400 mg of bezafibrate or 200 mg of fenofibrate was performed. Study subjects were 14 dyslipidemia with impaired glucose tolerance or type 2 diabetes mellitus (61 ± 16 years, body mass index (BMI) 26 ± 3 kg/m^2, total cholesterol (TC) 219 ± 53 mg/dL, triglyceride (TG) 183 ± 83 mg/dL, high-density lipoprotein-cholesterol (HDL-C) 46 ± 8 mg/dL, fasting plasma glucose 133 ± 31 mg/dL and HbA1c 6.2 ± 0.8%). Subjects were given either bezafibrate or fenofibrate for 8 weeks, discontinued for 4 weeks and then switched to the other fibrate for 8 weeks. Circulating PCSK9 levels and other metabolic parameters, including adiponectin, leptin and urine 8-hydroxy-2′-deoxyguanosine (8-OHdG) were measured at 0, 8, 12 and 20 weeks.
Results: Plasma PCSK9 concentrations were significantly increased (+39.7% for bezafibrate and +66.8% for fenofibrate, $p < 0.001$) in all patients except for one subject when treated with bezafibrate. Both bezafibrate and fenofibrate caused reductions in TG (−38.3%, $p < 0.001$ *vs.* −32.9%, $p < 0.01$) and increases in HDL-C (+18.0%, $p < 0.001$ *vs.* +11.7%, $p < 0.001$). Fenofibrate significantly reduced serum cholesterol levels (TC, −11.2%, $p < 0.01$; non-HDL-C, −17.3%, $p < 0.01$; apolipoprotein B, −15.1%, $p < 0.01$), whereas bezafibrate significantly improved glucose tolerance (insulin, −17.0%, $p < 0.05$) and metabolic markers (γ-GTP, −38.9%, $p < 0.01$; adiponectin, +15.4%, $p < 0.05$; urine 8-OHdG/Cre, −9.5%, $p < 0.05$).
Conclusion: Both bezafibrate and fenofibrate increased plasma PCSK9 concentrations. The addition of a PCSK9 inhibitor to each fibrate therapy may achieve beneficial cholesterol lowering along with desirable effects of respective fibrates.

1. Introduction

Proprotein convertase subtilisin kexin type 9 (PCSK9) is a member of the subtilisin-like serine convertase superfamily made and secreted by the liver into the plasma. Secreted PCSK9 regulates plasma LDL-cholesterol (LDL-C) levels by directing cell-surface LDL receptors (LDLR) to the lysosomes for degradation, resulting in reduced clearance and accumulation of LDL-C in the circulation [1–3]. Statins have been known to increase the nuclear translocation of sterol-regulatory element binding protein-2 (SREBP-2), which activates not only the LDLR but also PCSK9 gene expression [4–6]. Subsequently, statins increases serum PCSK9 levels [5–8] and this increment may attenuate the LDL-C lowering effect of statins. It may in a part explain the rule of 6% for statins, which indicates that each doubling of the statin dose results in only about a 6% further decrease in LDL-C.

Unlike statin treatment, the association of fibrate treatment with PCSK9 is less clear. Recently, it was shown that fenofibrate

* Corresponding author. Tel.: +81 76 265 2268, fax: +81 76 234 4271.
E-mail address: junji@med.kanazawa-u.ac.jp (J. Kobayashi).

0021-9150/$ – see front matter © 2011 Elsevier Ireland Ltd. All rights reserved.
doi:10.1016/j.atherosclerosis.2011.02.012

suppressed PCSK9 expression at the promoter level and reduced statin-induced PCSK9 secretion in vitro [9], whereas, fenofibrate did not suppress and rather increased circulating PCSK9 level in several in vivo studies [8,10,11]. Bezafibrate is another widely used fibrate, and both of which have substantial triglyceride (TG)-reducing-effect and high-density lipoprotein cholesterol (HDL-C)-raising effect. Bezafibrate is a pan-agonist for peroxisome proliferator-activated receptor (PPAR)-α, β and δ and fenofibrate is a more selective ligand for PPAR-α [12], and thus the effects of these drugs varies in several aspects. To the best of our knowledge, there is no previous study on the effect of bezafibrate treatment on PCSK9.

In this background, we directly compared the effect of fenofibrate and bezafibrate treatment on plasma PCSK9 and other metabolic parameters related to insulin sensitivity in crossover design.

2. Materials and methods

2.1. Study subjects

To assess the effects of bezafibrate and fenofibrate on plasma PCSK9, glucose tolerance and lipid metabolism, we enrolled 14 dyslipidemic subjects with impaired glucose tolerance or type 2 diabetes mellitus (T2DM); 11 men and 3 women, age 60.5 ± 15.6 years, body mass index (BMI) 26.0 ± 3.1 kg/m^2, total cholesterol (TC) 219.0 ± 52.7 mg/dL, TG 183.0 ± 82.9 mg/dL, HDL-C 45.9 ± 8.4 mg/dL, fasting plasma glucose 133.0 ± 30.8 mg/dL and HbA1c 6.22 ± 0.85%. Among them, 5 were on anti-diabetic drug and 7 were on anti-hypertensive drug, and the dosages of these treatments were not changed during the study period. None of the subjects were on insulin treatment or anti-lipid drugs other than fibrates.

Exclusion included: age > 75 years, BMI > 30 kg/m^2, HbA1c > 7.5%, serum TG level > 400 mg/dL, abnormal liver or muscle enzymes, creatinemia, habitual alcohol intake > 3 standard drink/day or endocrinological disorder.

2.2. Study protocol

This study was conducted as open randomized crossover design to compare the efficacy and the safety of bezafibrate and fenofibrate. All the participants were outpatients and were divided into two groups by envelope-method (Table 1). The group 1 (6 male, average age of 63.0 years) was started with 400 mg/day of bezafibrate, while the group 2 (5 male and 3 female, average age of 58.6 years) with 200 mg/day of fenofibrate. Any lipid lowering agents had been discontinued at least for 4 weeks before the study. The first phase was continued for 8 weeks, then bezafibrate or fenofibrate was discontinued for 4 weeks, and then subsequently patients were switched to the other fibrate treatment and continued it for another 8 weeks.

A statement of institutional approval of the study in accordance with the Declaration of Helsinki was provided, and written informed consent was obtained from all of the participants in this study.

2.3. Measurement of the laboratory data

Blood samples were obtained after an overnight fasting, and centrifuged at 4 °C. Serum TC and TG were determined by enzymatic method, and HDL-C levels were measured by a polyamine-polymer/detergent method (Daiichi Pure Chemical, Tokyo, Japan) as described elsewhere [13]. LDL-C levels were calculated using the Friedewald formula. Apolipoprotein A1, A2, B, C2, C3 and E were determined as described previously [14]. Plasma PCSK9 concentrations were determined using a commercially available quantitative sandwich enzyme-linked immunosorbent assay (ELISA) kit targeting human PCSK9 following the manufacturer instructions (Circulex CY-8079, CycLex Co, Nagano, Japan). The plasma levels of adiponectin and leptin were determined by the previously reported methods [15,16]. The levels of Urinary 8-hydroxy-2′-deoxyguanosine (8-OHdG) were determined using an ELISA kit (Stressgen, British Columbia, Canada) in accordance with the manufacturer's instructions. Other laboratory values, including fasting plasma glucose, HbA1c, glycoalbumin, aspartate aminotransferase (AST), alanine aminotransferase (ALT) and gamma-glutamyl transpeptidase (γ-GTP) were obtained using commercially available kits with an autoanalyzer. Serum insulin levels were determined by enzyme immunoassay. Uric Acid was determined using the uricase method. Homeostasis model assessment-insulin resistance (HOMA-IR) was calculated using the formula: HOMA-IR = (fasting insulin in mU/l × fasting plasma glucose in mg/dL)/405.

Table 1
Profile for the study subjects in group 1 and 2.

	Group 1	Group 2
Number of subjects, *n* (M/F)	6 (6/0)	8 (5/3)
Age, years	63.0 ± 18.2	58.6 ± 14.3
Body mass index, kg/m^2	26.3 ± 3.1	25.9 ± 3.3
Risk Factors, *n* (%)		
Hypertension	2 (33.3)	4 (50)
Diabetes mellitus	3 (50)	5 (62.5)
Current smoking	0 (0)	1 (12.5)
CAD	0 (0)	0 (0)
Medication, *n* (%)		
Anti-hypertensive[a]	3 (50)	4 (50)
CCBs	2 (33.3)	1 (12.5)
ARBs	2 (33.3)	4 (50)
ACE inhibitors	0 (0)	1 (12.5)
Diuretics	1 (16.7)	0 (0)
Beta blockers	0 (0)	1 (12.5)
Anti-diabetes	3 (33.3)	2 (25)
Sulfonylurea	1 (16.7)	1 (12.5)
Alpha-GI	1 (16.7)	1 (12.5)
Glinide	1 (16.7)	0 (0)

Abbreviations: CCBs, calcium channel blockers; ARBs, angiotensin II receptor blockers; ACE, angiotensin-converting enzyme; Alpha-GI, alpha-glucosidase inhibitors.
Values for age and body mass index are shown as mean ± SD.
The numbers in the parentheses show percent.
[a] Some of the patients had received more than one agent for hypertension.

2.4. Statistics

All values in the text and tables are expressed as mean ± SD unless otherwise stated. Effects of each drug therapy on each variable were analyzed by means of paired *t*-test. Treatment effects were compared between two fibrates using a mixed model ANOVA. Linear correlations were analyzed using Pearson's correlation coefficient analysis. All statistical analyses were performed with PASW statistics 17.0.3 (SPSS, Chicago, IL). A *p*-value of less than 0.05 was considered to indicate statistical significance.

3. Results

3.1. Characteristics of study subjects at baseline were similar in both groups

In either group 1 or 2, parameters related to lipid, glycemic control and other markers did not significantly differ before starting either fibrate. For further analysis, the data from both groups were combined and analyzed in detail. Pre- and post-treatment values of each parameter were shown in Table 2. There were no variables that would indicate carry-over and time-dependent effects.

Table 2
Effects of bezafibrate and fenofibrate treatment on metabolic parameters.

	Bezafibrate		Fenofibrate		Mixed model ANOVA *p* value
	Pre-treatment	Post-treatment	Pre-treatment	Post-treatment	
Body mass index, kg/m^2	26.2 ± 3.2	26.0 ± 3.3	26.0 ± 3.0	26.0 ± 3.1	0.414
AST, U/L	34.6 ± 19.6	36.4 ± 18.5	32.8 ± 21.1	32.7 ± 14.5	0.800
ALT, U/L	47.1 ± 35.8	36.9 ± 21.4	42.7 ± 33.0	35.4 ± 21.0	0.765
γGTP, U/L	59.1 ± 43.8	36.1 ± 22.7**	55.6 ± 40.1	41.8 ± 23.9	0.465
Uric Acid, mg/dL	5.6 ± 1.3	6.0 ± 1.7*	5.9 ± 1.4	4.0 ± 1.3***	<0.001†††
Total cholesterol, mg/dL	211.1 ± 51.5	209.6 ± 44.2	216.3 ± 49.1	192.1 ± 40.4**	0.034†
Triglyceride, mg/dL	196.4 ± 81.3	121.1 ± 52.7**	179.4 ± 77.1	120.3 ± 39.5**	0.511
HDL-cholesterol, mg/dL	44.4 ± 9.1	52.4 ± 10.6***	45.3 ± 9.2	50.6 ± 11.2***	0.097
LDL-cholesterol, mg/dL	127.5 ± 47.0	133.0 ± 36.8	135.1 ± 44.3	117.4 ± 33.5	0.032†
Non-HDL-cholesterol, mg/dL	166.8 ± 47.6	157.2 ± 41.0	171.0 ± 44.3	141.5 ± 36.5**	0.058
PCSK9, ng/mL	272.0 ± 62.0	380.0 ± 84.8***	266.7 ± 56.6	444.8 ± 101.3***	0.077
Apo A1, mg/dL	128.8 ± 18.1	141.4 ± 22.0***	130.7 ± 18.4	141.8 ± 19.4***	0.696
Apo A2, mg/dL	29.8 ± 4.3	40.7 ± 5.6***	30.3 ± 5.1	40.7 ± 4.9***	0.742
Apo B, mg/dL	107.4 ± 28.0	104.5 ± 24.2	112.2 ± 25.0	95.3 ± 21.6**	0.018†
Apo C2, mg/dL	5.9 ± 2.7	5.2 ± 2.3	6.0 ± 3.1	4.9 ± 1.9	0.412
Apo C3, mg/dL	10.9 ± 3.7	8.8 ± 3.0**	11.2 ± 4.2	8.5 ± 2.3**	0.548
Apo E, mg/dL	5.3 ± 1.7	4.6 ± 1.0*	5.6 ± 2.3	4.9 ± 3.2	1.000
Plasma glucose, mg/dL	132.0 ± 28.8	121.6 ± 24.9	126.1 ± 25.2	124.9 ± 28.6	0.246
HbA1c, %	6.24 ± 0.83	6.18 ± 0.78	6.03 ± 0.71	6.25 ± 0.77*	0.053
Glycoalbumin, %	17.5 ± 4.2	16.8 ± 3.7	16.6 ± 3.0	17.5 ± 4.1	0.011†
Insulin, mU/L	9.4 ± 5.0	7.8 ± 3.4*	9.4 ± 5.6	8.8 ± 3.9	0.278
HOMA-IR	2.84 ± 1.29	2.32 ± 1.06*	2.90 ± 1.86	2.79 ± 1.65	0.241
Leptin, ng/mL	7.4 ± 5.0	7.3 ± 6.6	7.8 ± 7.6	8.3 ± 6.4	0.553
Adiponectin, μg/mL	6.5 ± 2.7	7.5 ± 3.1*	6.9 ± 3.1	7.1 ± 3.6	0.187
Urine 8-OHdG/Cre, ng/mgCre	10.5 ± 2.6	9.5 ± 1.7*	10.0 ± 2.7	9.6 ± 2.0	0.471

Abbreviations: AST, aspartate aminotransferase; ALT, alanine aminotransferase; γ-GTP, gamma-glutamyl transpeptidase; HDL, high density lipoprotein; LDL, low density lipoprotein; Apo, apolipoprotein; HOMA-IR, homeostasis model assessment-insulin resistance; 8-OHdG, 8-hydroxy-2′-deoxyguanosine.
Values are shown as mean ± SD.
* $p < 0.05$ *vs.* pre-treatment value.
** $p < 0.01$ *vs.* pre-treatment value.
*** $p < 0.001$ *vs.* pre-treatment value.
† $p < 0.05$ *vs.* bezafibrate treatment.
††† $p < 0.001$ *vs.* bezafibrate treatment.

3.2. Bezafbrate decreased γ-GTP, whereas fenofibrate showed better effect on uric acid than bezafibrate

There was no significant change in BMI and AST between values before and after treatment. There was a slight but not significant reduction in ALT during either treatment. γ-GTP decreased with bezafibrate ($p < 0.01$), but not with fenofibrate. Uric acid decreased with fenofibrate ($p < 0.001$), whereas slightly increased with bezafibrate ($p < 0.05$), and the effects of two fibrates on uric acid were significantly different from each other ($p < 0.001$).

3.3. Fenofibrate had better effects on cholesterol metabolism than bezafibrate, though both fibrates increased plasma PCSK9 levels

Plasma PCSK9 levels were increased in 13 of 14 subjects with bezafibrate (+39.7%, $p < 0.001$, Fig. 1A) and in all subjects with fenofibrate (+66.8%, $p < 0.001$, Fig. 1B).

Both bezafibrate and fenofibrate treatments were associated with reductions in serum TG (bezafibrate, $p < 0.001$; fenofibrate $p < 0.01$), and increases in HDL-C ($p < 0.001$ for either of treatment). There were significant reductions in TC ($p < 0.01$), apolipoprotein B ($p < 0.01$) and non-HDL-C ($p < 0.01$), and slight decrease in LDL-C during fenofibrate treatment, whereas bezafibrate did not produce reductions in these parameters. As a result, cholesterol lowering effect of fenofibrate were significantly stronger than that of bezafibrate ($p < 0.05$ for TC, LDL-C and apolipoprotein B).

Serum levels of apolipoprotein A1 and A2 were significantly increased ($p < 0.001$) and those of apolipoprotein C3 were significantly decreased ($p < 0.01$) during both of these treatments. Apolipoprotein E level was slightly but significantly decreased during bezafibrate treatment ($p < 0.05$). There were no significant changes in apolipoprotein C2 levels between values before and after fenofibrate or bezafibrate treatments.

3.4. Bezafibrate had better effects on glucose tolerance than fenofibrate

Changes in plasma glucose and glycoalbumin were not significant during either treatment. Fenofibrate was associated with a slight but significant increase in HbA1c ($p < 0.05$) whereas bezafibrate was not. Insulin level and HOMA-IR significantly decreased with bezafibrate ($p < 0.05$) but not with fenofibrate.

3.5. Bezafibrate improved serum adiponectin level and oxidative stress marker

Bezafibrate but not fenofibrate was associated with a significant increase in serum adiponectin ($p < 0.05$) and with a significant decrease in urine 8-OHdG/Cre ($p < 0.05$). Serum leptin did not significantly alter in either treatment.

3.6. Associations of plasma PCSK9 with cholesterol and several metabolic markers

As shown in Table 3, circulating PCSK9 levels were significantly correlated with TC ($r = 0.477$, $p = 0.01$), LDL-C ($r = 0.501$, $p < 0.01$), non-HDL-C ($r = 0.453$, $p < 0.05$), BMI ($r = 0.377$, $p < 0.05$), γGTP ($r = 0.376$, $p < 0.05$), plasma glucose ($r = -0.426$, $p < 0.05$), HbA1c ($r = -0.468$, $p < 0.05$), glycoalbumin ($r = -0.563$, $p < 0.01$), insulin ($r = 0.507$, $p < 0.01$), HOMA-IR ($r = 0.396$, $p < 0.05$) and leptin ($r = 0.416$, $p < 0.05$) at baseline levels. When analyzed using absolute or percent change value for each variable during the treatment, no significant associations were observed in the present study.

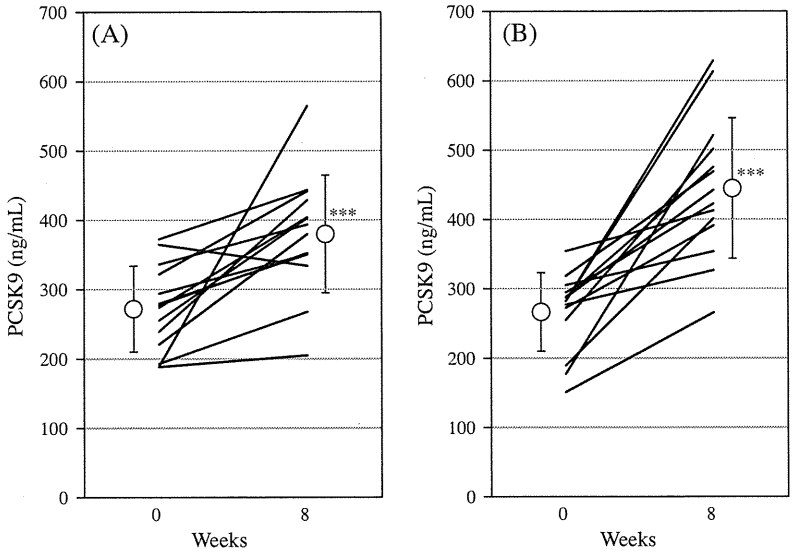

Fig. 1. Changes in circulating PCSK9 concentrations in response to 8 weeks of treatment with (A) 400 mg of bezafibrate per day or (B) 200 mg of fenofibrate per day. Open circles represent means of 14 subjects and bars SD. ***$p < 0.001$ *vs.* pre-treatment value.

4. Discussion

The main finding of the present study is that all subjects with fenofibrate treatment and all but one subject with bezafibrate treatment showed increases in their circulating PCSK9 levels. The degree of increase in PCSK9 tended to be higher in fenofibrate treatment than in bezafibrate treatment (+66.8% *vs.* +39.7%, $p = 0.077$). This is the first study investigating the differences between bezafibrate and fenofibrate in their effects on circulating PCSK9 level and other metabolic parameters related to insulin resistance and oxidative stress in Japanese hyperlipidemic subjects.

As observed in previous reports [17–19], we found that plasma PCSK9 levels positively correlated with TC, LDL-C, non-HDL-C, BMI, γGTP, insulin and HOMA-IR at baseline levels in subjects with impaired glucose tolerance or T2DM. On the other hand, fasting plasma glucose was negatively correlated with plasma PCSK9 levels in our study on impaired glucose tolerance or T2DM, which does not appear to be consistent with these reports on non-diabetic patients. Very recently, however, it was shown that PCSK9 knockout mice had higher glucose and lower insulin levels than wild-type mice [20], suggesting some association of PCSK9 with increasing insulin leading to lowering of plasma glucose. This may in part explain the negative correlation of PCSK9 with plasma glucose and HbA1c in our study.

Table 3
Relationships of PCSK9 to metabolic parameters at baseline.

	r	*p*
Total cholesterol	0.477	0.010*
Triglyceride	−0.132	0.504
HDL-cholesterol	0.349	0.069
LDL-cholesterol	0.501	0.007**
Non-HDL-cholesterol	0.453	0.016*
Body mass index	0.377	0.048*
AST	0.188	0.337
ALT	0.326	0.090
γGTP	0.376	0.049*
Uric acid	0.179	0.382
Plasma glucose	−0.426	0.024*
HbA1c	−0.468	0.016*
Glycoalbumin	−0.563	0.002**
Insulin	0.507	0.008**
HOMA-IR	0.396	0.045*
Leptin	0.416	0.028*
Adiponectin	0.235	0.229
Urine 8-OHdG/Cre	0.019	0.927

Abbreviations as in Table 2.
* $p < 0.05$.
** $p < 0.01$.

Bezafibrate and fenofibrate have some evidence of preventing coronary artery disease in Bezafibrate Infarction Prevention (BIP) [21,22] and Fenofibrate Intervention and Event Lowering in Diabetes (FIELD) Study [23], respectively. Our present data indicate that fenofibrate treatment (200 mg per day for 8 weeks) produced more favorable effects on cholesterol metabolism than did bezafibrate treatment (400 mg per day for 8 weeks) with regard to lower TC, non-HDL-C, LDL-C and apolipoprotein B levels. Circulating PCSK9 protein levels were significantly increased by either of these two fibrates. Previous reports showed conflicting findings on the effect of fenofibrate on PCSK9. Kourimate et al. demonstrated that PPAR-α activation resulted in the repression of PCSK9 promoter activity, and in the up-regulation of PC5/6A and furin, which degrade PCSK9 [9]. To our knowledge, two clinical studies suggest that fenofibrate treatment was associated with decrease in PCSK9 levels [24,25]. Lambert et al. [24] reported that fenofibrate 200 mg/day was associated with decrease (−8.5%, $p = 0.041$) in PCSK9 level in diabetic patients and Chan et al. [25] showed fenofibrate 145 mg/day was associated with decrease (−13%, $p < 0.05$) in statin treated T2DM subjects. In contrast to these reports, Mayne et al. and Troutt et al. represented an increase in circulating PCSK9 level after fenofibrate treatment with 200 mg/day in dyslipidemic patients (+17%, $p = 0.031$ and +25%, $p < 0.01$, respectively) [8,10], although the precise mechanism contributing to these increases remains to be clarified. Furthermore, Costet et al. reported that 6 weeks of treatment with either 10 mg/day atorvastatin or 160 mg/day fenofibrate increased PCSK9 levels (+14%, $p = 0.01$ and +26%, $p < 0.01$, respectively) in T2DM subjects, with no additive effect after 6 weeks of combined therapy [11]. In our study, the effect of fenofibrate treatment with 200 mg/day on plasma PCSK9 level was more prominent (+66.8%) than these reports and was even higher than previously reported value of high dose (80 mg) atorvastatin treatment (+47%) [26], although study population and duration of the treatment were different.

In patients with T2DM, insulin resistance inhibits catabolism of remnant lipoproteins by reducing lipoprotein lipase (LPL) activity, contributing to the development of hypertriglyceridemia and

low HDL-C [27–29]. The present data indicate that bezafibrate and fenofibrate had equivalent efficacy on TG and HDL-C improvement in subjects with hyperglycemia. As a PPAR-α agonists, these fibrates improve triglyceride and HDL-C concentrations by enhancing β-oxidation of fatty acids and LPL activity, increasing production of the components of HDL (apolipoproteins A1 and A2), and reducing production of the inhibitor of LPL activity (apolipoprotein C3) [30–34], while enhancing cholesterol efflux from the liver [35]. Several reports [8,10] suggest that these effects of PPAR-α on cholesterol and lipoprotein metabolism may lead indirectly to decrease hepatic intracellular cholesterol levels, and thus result in a secondary increase in PCSK9 expression and secretion. Costet et al. reported that one-day administration of atorvastatin increased PCSK9 levels whereas that of fenofibrate did not [11], which might support the indirect slower effect of PPAR-α agonist on PCSK9 expression.

PPAR-γ is another target of bezafibrate and is expected to have effects on glucose metabolism and insulin resistance [36]. Several previous studies have indicated that bezafibrate treatment could be associated with improvement of glycemic control in diabetic subjects [37,38] or with delay of the onset of T2DM [39,40]. As for fenofibrate treatment, on the other hand, there are conflicting reports on its effect on glycemic control [41,42]. In our previous study [43], fasting plasma glucose level was unchanged after 8 weeks of treatment with fenofibrate, which is consistent with the present study. Of note, the very recent retrospective cohort study using data from routine medical practice in the United Kingdom [44] has shown that compared to fenofibrate, bezafibrate was associated with a particularly low hazard for the occurrence of T2DM (HR 0.41, 95% CI 0.29, 0.58). Indeed, our present findings suggest that bezafibrate is more desirable than fenofibrate concerning serum insulin level and HbA1c.

The mechanism by which the degree of PCSK9 increases was more modest in bezafibrate than in fenofibrate is not clarified yet. Costet et al. reported that insulin increased hepatic PCSK9 mRNA expression in rodent primary hepatocytes and in vivo during a hyperinsulinemic–euglycemic clamp in mice [45]. This finding combined with our present result that insulin level positively correlated with plasma PCSK9 level at baseline and that insulin level was decreased with bezafibrate but not with fenofibrate may in part explain the more modest increase in PCSK9 levels produced by the former than the latter.

In addition to the effect on glycemic control, these fibrates may have beneficial effects on adipocytokines, such as leptin, which positively correlated with PCSK9 in the present study, and adiponectin [41,46–49]. Damci et al. showed a reduction in leptin levels with fenofibrate treatment (250 mg/day for 3 months) [41], whereas no significant change in leptin levels was observed in either fibrate treatment in the present study with a shorter duration. For the effect of fibrate treatment on serum adiponectin, the present finding that fenofibrate did not increase serum adiponectin is consistent with our previous study [43], although some studies have shown associations of fenofibrate treatment with adiponectin increase in humans [46,47]. On the other hand, bezafibrate treatment was associated with an increase in serum adiponectin in the present study. Indeed, there are several previous studies linking bezafibrate to an increase in serum adiponectin in patients enrolled in the BIP study [48] and in spontaneous T2DM model (Otsuka Long-Evans Tokushima Fatty; OLETF) rats [49]. Hiuge et al. also reported that bezafibrate and fenofibrate significantly increased adiponectin levels in mice and 3T3-L1 adipocytes [48].

For the association between fibrate and liver function, there is a report linking bezafibrate treatment to an improvement of γ-GTP in subjects with chronic liver disease [50], which is compatible with the present finding although subjects did not have chronic liver disease in our study. Consistent with the report by Cariou et al. [18], γ-GTP positively correlated with PCSK9 at baseline in our study, and thus the significant decrease in γ-GTP only with bezafibrate might be related to the milder increase in circulating PCSK9 levels with bezafibrate than fenofibrate. A significant reduction in uric acid levels by fenofibrate in the present study is consistent with previous report [51], whereas there is no previous report on the effect of bezafibrate treatment on uric acid.

Angiopathy of T2DM has a complex etiology that may involve the effects of hyperlipidemia and oxidative stress on endothelial function. Similar to certain types of lipid lowering agents such as probucol and atorvastatin [52], we observed beneficial effect of bezafibrate to produce significant decreases in urine 8-OHdG/Cre, which has been recognized as an important oxidative stress marker.

One of the limitations of our study is the small sample size. However, the study was accomplished in the cross over design, making it possible to investigate the effect of bezafibrate and fenofibrate treatments in the same subjects and thereby enabling to exclude the possibility of study subject bias. Moreover, the results were clear and convincing especially in PCSK9 changes during fibrate treatment.

In conclusion, both bezafibrate and fenofibrate cause considerable increase in plasma PCSK9 in hyperlipidemic subjects with the former in more modest manner. We suggest that in the treatment of hyperlipidemic subjects, the addition of a PCSK9 inhibitor to each fibrate therapy may achieve beneficial cholesterol lowering along with desirable effects of respective fibrates.

Disclosure

The contents of this paper have not been published or communicated elsewhere. The authors have no relationships with companies regarding a financial interest in the information contained in this paper.

Acknowledgement

This work was partly supported by Health and Labor Sciences Research Grants from the Ministry for Health, Labor and Welfare in Japan.

References

[1] Zhang DW, Lagace TA, Garuti R, et al. Binding of proprotein convertase subtilisin/kexin type 9 to epidermal growth factor-like repeat A of low density lipoprotein receptor decreases receptor recycling and increases degradation. J Biol Chem 2007;282:18602–12.
[2] Qian YW, Schmidt RJ, Zhang Y, et al. Secreted PCSK9 downregulates low density lipoprotein receptor through receptor-mediated endocytosis. J Lipid Res 2007;48:1488–98.
[3] Lagace TA, Curtis DE, Garuti R, et al. Secreted PCSK9 decreases the number of LDL receptors in hepatocytes and in livers of parabiotic mice. J Clin Invest 2006;116:2995–3005.
[4] Rashid S, Curtis DE, Garuti R, et al. Decreased plasma cholesterol and hypersensitivity to statins in mice lacking Pcsk9. Proc Natl Acad Sci U S A 2005;102:5374–9.
[5] Dubuc G, Chamberland A, Wassef H, et al. Statins upregulate PCSK9, the gene encoding the proprotein convertase neural apoptosis-regulated convertase-1 implicated in familial hypercholesterolemia. Arterioscler Thromb Vasc Biol 2004;24:1454–9.
[6] Dong B, Wu M, Li H, et al. Strong induction of PCSK9 gene expression through HNF1alpha and SREBP2: mechanism for the resistance to LDL-cholesterol lowering effect of statins in dyslipidemic hamsters. J Lipid Res 2010;51:1486–95.
[7] Careskey HE, Davis RA, Alborn WE, Troutt JS, Cao G, Konrad RJ. Atorvastatin increases human serum levels of proprotein convertase subtilisin/kexin type 9. J Lipid Res 2008;49:394–8.
[8] Mayne J, Dewpura T, Raymond A, et al. Plasma PCSK9 levels are significantly modified by statins and fibrates in humans. Lipid Health Dis 2008;7:22.
[9] Kourimate S, Le May C, Langhi C, et al. Dual mechanisms for the fibrate-mediated repression of proprotein convertase subtilisin/kexin type 9. J Biol Chem 2008;283:9666–73.
[10] Troutt JS, Alborn WE, Cao G, Konrad RJ. Fenofibrate treatment increases human serum proprotein convertase subtilisin kexin type 9 levels. J Lipid Res 2010;51:345–51.